Universidade de Aveiro
2008

Departamento de Física

Magda Catarina Ferreira de Sousa

Análise da Variabilidade da Temperatura da Água no Canal do Espinheiro

Water Temperature Variability Analysis along the Espinheiro Channel

Universidade de Aveiro
2008

Departamento de Física

Magda Catarina Ferreira de Sousa

Análise da Variabilidade da Temperatura da Água no Canal do Espinheiro

Water Temperature Variability Analysis along the Espinheiro Channel

Dissertação apresentada à Universidade de Aveiro para cumprimento dos requisitos necessários à obtenção do grau de Mestre em Meteorologia e Oceanografia Física, realizada sob a orientação científica do Prof. Doutor João Miguel Dias, Professor Auxiliar do Departamento de Física da Universidade de Aveiro e co-orientação do Doutor Nuno Vaz, investigador de pós-doutoramento do Instituto Superior Técnico.

Este estudo foi desenvolvido no âmbito do projecto AMDRAPHYD (POCI/AMB/57928/2004) financiado pela Fundação para a Ciência e Tecnologia (FCT) e pelo FEDER.

o júri

presidente

Prof. Doutor Paulo Manuel Cruz Alves da Silva
Professor auxiliar do Departamento de Física da Universidade de Aveiro

Prof. Doutor João Miguel Sequeira Silva Dias
Professor auxiliar do Departamento de Física da Universidade de Aveiro

Doutor Nuno Alexandre Firmino Vaz
Investigador de pós-doutoramento do Instituto Superior Técnico

Prof. Doutora Maria Inés Alvarez Fernández
Professora associada do Departamento de Física Aplicada, Facultad de Ciências de Ourense, Universidade de Vigo (Grupo de Física Oceanográfica y de Costas)

acknowledgements

In this section I only mention the most relevant people, but I would like to thank all who contributed positively in my work, in particular my two advisors Prof. Doutor João Miguel Dias and Doutor Nuno Vaz, without whom this work would not have been possible.

I have also benefited from very valuable comments and help by Ana Pires at different stages of this work.

Finally, I also would like to thank my parents and Daniel, for their support and affection.

Palavras-chave temperatura da água; análise; canal do Espinheiro; Ria de Aveiro

Resumo

O canal do Espinheiro é um dos quatro principais canais da Ria de Aveiro, fazendo a ligação entre o Rio Vouga e o Oceano Atlântico. Nesta zona é onde se dá a mistura entre a água salgada proveniente do oceano e a água doce de origem fluvial. Para fazer a monitorização da temperatura da água no Canal do Espinheiro foi utilizada uma nova tecnologia que consiste num cabo de fibra óptica longitudinal de 10 km de extensão, com 18 sensores de temperatura espaçados de 500 m, desde a embocadura até à foz do Rio Vouga.

Resultados de um ano de monitorização da temperatura da água permitiram estudar a sua variabilidade espacial e temporal em função de dois forçamentos principais: maré e condições meteorológicas.

A evolução temporal longitudinal da temperatura da água foi estudada, tendo sido aplicadas técnicas matemáticas, tais como: análise espectral, análise espectral cruzada e funções empíricas ortogonais (EOFs).

A análise espectral mostra picos de maior energia que surgem nas frequências semi-diurnas e diurnas. Estas frequências podem estar relacionadas com a variação diurna da temperatura do ar e da maré, mostrando a importância das variáveis meteorológicas na modulação da temperatura da água em regiões pouco profundas. A análise espectral cruzada permitiu avaliar o desfasamento temporal entre a temperatura da água e do ar, que varia conforme a profundidade do local. Também permitiu observar que a maré tem uma grande influência na distribuição da temperatura da água, nomeadamente perto da embocadura da laguna. As EOFs mostram que a variabilidade da temperatura da água pode ser explicada maioritariamente pela primeira componente, que está relacionada com a variação anual da temperatura do ar.

Os resultados mostram que os dois forçamentos principais (maré e condições meteorológicas) determinam a temperatura da água no interior do canal do Espinheiro. Verifica-se ainda que a distribuição da temperatura da água é influenciada também pela variação sazonal das condições meteorológicas e pelas variações de profundidade do canal, que apresenta zonas de reduzida profundidade.

keywords water temperature; analysis; Espinheiro channel; Ria de Aveiro

Abstract

The Espinheiro channel is one of the four main branches of Ria de Aveiro, establishing the connection between the Vouga River and the Atlantic Ocean. This zone is where occurs the mixing between the salt water from the ocean and the freshwater from fluvial origin. In order to monitoring the water temperature in the Espinheiro channel a new technology was used, consisting on an optical-fibre longitudinal cable 10 km long with 18 temperature sensors separated by 500 m, from the mouth of the lagoon to the mouth of Vouga River. Results of a one year monitoring of water temperature permitted to study its spatial and temporal variability in terms of two major forcing: tides and meteorological conditions.

The temporal evolution of the longitudinal water temperature was studied, and mathematical techniques, such as spectral analysis, cross-spectral analysis and Empirical Orthogonal Functions (EOFs) were applied to the data.

The spectral analysis shows high energy peaks in both semidiurnal and diurnal frequencies. These frequencies may be related to the daily variation and tidal forcing, demonstrating the importance of the meteorological variables in the modulation of the water temperature in shallow areas. The cross-spectral analysis permitted to evaluate the time lag between the water and air temperature, which varies depending on the local depth. It also permitted to observe that the tide has a great influence on the water temperature distribution, particularly near the mouth of the lagoon. EOFs show that the variability of the water temperature can be explained by the first component, which is closely related to the annual variation of the air temperature.

The results show the importance of the two major forcings (tides and meteorological conditions) that determine the water temperature within the Espinheiro channel. It can also be observed that the water temperature distribution is also influenced by the seasonal variation of meteorological conditions and by the channel's depth variation, which presents very shallow areas.

Contents

List of Figures

List of Tables

1 Introduction

Water temperature plays a key environmental, ecological and morphological role within an estuary. "*An estuary is defined as a semi-enclosed coastal body of water which has a free connection with the open sea and within which sea water is measurably diluted with freshwater derived from land drainage*"(Cameron and Pritchard, 1963). Accordingly, an estuary is a zone of transition between the marine-dominated systems (ocean) and the upland river systems.

Water temperature influences the rate of plant photosynthesis (Wang *et al*., 2007), the metabolic rates of aquatic organisms (Atkinson *et al*., 1987), and the sensitivity of organisms to toxic wastes, parasites, and diseases (USEPA, 1997). As example, water temperature increases, the capacity of water to hold dissolved oxygen becomes lower.

Estuarine water temperature in temperate regions is primarily a function of the temperatures of influent streams, rivers, the ocean, and tidal stage (Reid and Wood, 1976). Estuarine water temperature also varies with air temperature, depth, which leads to vertical temperature gradients, changes in the amount of freshwater, and the extent to which freshwater is mixed with marine water by winds or tides. Also, discharges of "cooling" waters from power plants and municipal or industrial effluents are sources of thermal pollution in the coastal zone. Because most estuaries are shallow, there can be considerable diurnal and seasonal temperature variations (Kaplan *et al*., 2003).

In order to characterize the water temperature in coastal regions some studies have been performed: Aliani *et al*. (2004) applied the tidal harmonic analysis to identify the low frequencies in the temperature series at a marine shallow water hydrothermal vent in Milos Island. Harcourt-Baldwin and Diedericks (2006) studied the density currents in Tomales Bay (California) whose formation is controlled by tidal conditions, ocean temperature, wind, insolation and estuary depth; freshwater inflow at the head of the estuary had no impact on the density intrusions. Paraso and Valle-Levinson (1996) concluded that the barometric pressure and wind forcing were responsible for the horizontal water temperature gradient in the lower Chesapeake Bay. Uncles and Stephens (2001) studied the annual cycle of temperature and associated heat fluxes in the Tamar Estuary and concluded that the daily averaged heat transport towards the coastal zone closely followed the temperature difference between freshwater and coastal waters and was modulated by both

freshwater flow and spring-neap tidal variations. Newton and Mudge (2003) studied the temperature and salinity regimes in a shallow, mesotidal lagoon, the Ria Formosa (Portugal) and demonstrated that in areas inside of the lagoon there were different temperature and salinity characteristics compared to the inflowing coastal water, both in Winter and Summer. Thomas *et al*. (2002) concluded that the differences in sea surface temperature (SST) along the central coast of Maine (USA) in Summer are due to differences in residual circulation, freshwater input and flushing. Empirical Orthogonal Functions (EOFs) analysis was used to study the dominant patterns of SST variance in Delaware Bay (Keiner and Yan, 1997) and to study the SST variability off Northern and Central California from AVHRR Satellite Imagery (Armstrong, 1995).

In this work is studied the water temperature variability analysis along the Espinheiro Channel. The Espinheiro Channel is one of the four main branches of Ria de Aveiro, a mesotidal and shallow coastal lagoon located in the northwest coast of Portugal. This channel connects the major source of freshwater of the lagoon, the Vouga River, to the Atlantic Ocean, being ideal to perform studies such as the one proposed here. Ria de Aveiro provides natural conditions for harbor, navigation and recreation facilities and it is also a place of discharge of domestic and industrial wastes.

The fast and complex dynamics of Ria de Aveiro, along with its physical and biogeochemical importance has motivated several studies in the region, including: numerical modeling studies of its hydrodynamics (Dias, 2001; Sousa and Dias, 2007; Vaz *et al*., 2007). Previous hydrological characterizations of Ria de Aveiro (Dias *et al*., 1999; Vaz *et al*., 2005; Vaz and Dias, 2008) conclude that the lagoon can be considered as vertically homogeneous, except in very strong freshwater flows events, where the lagoon becomes weakly stratified. Several studies were performed to investigate topics such as the tidal propagation in the lagoon (Dias *et al*., 2000), the Lagrangian transport of particles (Dias *et al*., 2001) and sediment transport (Lopes *et al*., 2001). Abrantes *et al*. (2006) studied the suspended sediment concentration in different parts of the lagoon during tidal cycles which showed a significant spatial and temporal variability.

The characteristics of Ria de Aveiro, as well as of other estuarine systems, make permanent monitoring particularly important for its management. The use of conventional sampling technologies of physical parameters revealed to be very expensive and hard to use in high spatial and temporal scales. Water temperature is closely connected to many

biological and chemical processes in the estuary. For this reason, and because it is easily measured, temperature is commonly monitored. To monitor the water temperature there are various instruments, most of all based on the use of thermistors (type of resistor with resistance varying according to its temperature), but most are only used for short time periods (Vaz and Dias, 2008). Goto *et al*. (2003) used the WaDar temperature logger, which is a shelf-recording thermometer designed for long term temperature monitoring, in order to monitor hydrothermal activity. With the purpose of long term monitoring water temperature and without the need of regular human intervention, a new technology composed by an optical longitudinal cable integrating fibre Bragg grating sensors was developed and installed in the Espinheiro channel, in the frame of the research project Proteu (POCTI/MAR/15275/1999).

The objectives of this work are to study the water temperature variability along the channel that connects the ocean to the major freshwater input in the lagoon, evaluating the importance of the main forcing mechanisms: tides and meteorological conditions. The water temperature is monitored using the new technology referred above. The data under analysis consist in 18 annual time series of water temperature from sampling locations separated by 500 m, allowing the study of its spatial and temporal variability. The temporal evolution of the longitudinal water temperature gradients is studied and mathematical techniques such as the spectral and cross-spectral analysis, harmonic analysis and EOFs are applied to the data.

This work is divided into six sections. Section 2, includes the description of the study area. Section 3 contains short descriptions of the data and of the mathematical techniques applied to study the spatial, temporal and spatial-temporal variability of the water temperature. Section 4 shows the observations and environmental data used in this study. The results are discussed in Section 5. Section 6 summarizes the main conclusions and the future work suggestions.

2 Study area

Ria de Aveiro is a mesotidal shallow (mean depth of about 1 m relative to the local datum) vertically homogeneous lagoon with a very complex geometry located on the northwest Atlantic coast of the Iberian Peninsula, in Portugal (40º38'N, 8º45'W) (Figure 2.1). It is 45 km long and 10 km wide and covers an area of 83 km^2 at high tide (spring tide), which is reduced to 66 km^2 at low tide. It is characterized by narrow channels and by large areas of mud flats and salt marshes. The lagoon has four main channels: Mira and Ílhavo channels in its southern region, S. Jacinto channel in its northern region and the Espinheiro channel in the very complex central area of the lagoon. In order to simplify, the study area from the mouth up to the channel's head, close to the mouth of the Vouga River will be hereinafter referred as Espinheiro channel. The study area is approximately 11 km long, has an average width of 200 m and a mean depth, along its longitudinal axis, of about 10 m.

The tides in the Ria de Aveiro are semidiurnal, being M_2 and S_2 the most important constituents, representing more than 90% of the tidal energy (Dias *et al*., 1999). The estimated tidal prism for the lagoon's mouth at extreme spring and extreme neap is according to Dias (2001) 136.7×10^6 m^3 and 34.9×10^6 m^3, respectively. The estimated tidal prism for the real Espinheiro channel is about 40×10^6 at extreme spring tide and 15×10^6 m^3 at extreme neap tide (Dias, 2001). The total estimated freshwater input for the lagoon is very small (about 1.8×10^6 m^3 during tidal cycle) (Moreira *et al*., 1993) when compared to the tidal prism both at the mouth or at the beginning of Espinheiro channel.

Espinheiro channel may be considered the most important area of the Ria de Aveiro, because the strongest currents are observed here, reaching values higher than 2 ms^{-1}. The other channels are mainly shallow and tidal flat areas, contributing to a strong damping of currents (Vaz, 2007). The salinity ranges from fluvial (about 0 psu) to oceanic typical values (between 32 and 35 psu), depending on the freshwater inputs (Dias, 2001; Vaz *et al*, 2005). The hydrodynamic of the channel is largely dependent on the tidal wave characteristics and freshwater inputs variability.

The most important freshwater contribution is from Vouga River. Its mouth is located near the head of the study area and therefore its freshwater inflow is determinant in the establishment of the channel's physical patterns. When the river flow is low (less than

10 m^3s^{-1}) the water column is filled with salt water from the ocean until almost 8 km from the channel's mouth. When the river flow is higher than 100 m^3s^{-1} vertical stratification is established along the channel, and the freshwater from Vouga River extends its influence up to the channel's mouth. When the river flow is between 30 and 50 m^3s^{-1}, the channel can be divided into three deferent regions: a lower marine region where the thermohaline variables present oceanic values; an intermediate inner region where mixing between ocean and river water occurs and a upper fluvial region which is dominated by freshwater but is still subject to a semidiurnal tidal action (Vaz and Dias, 2008).

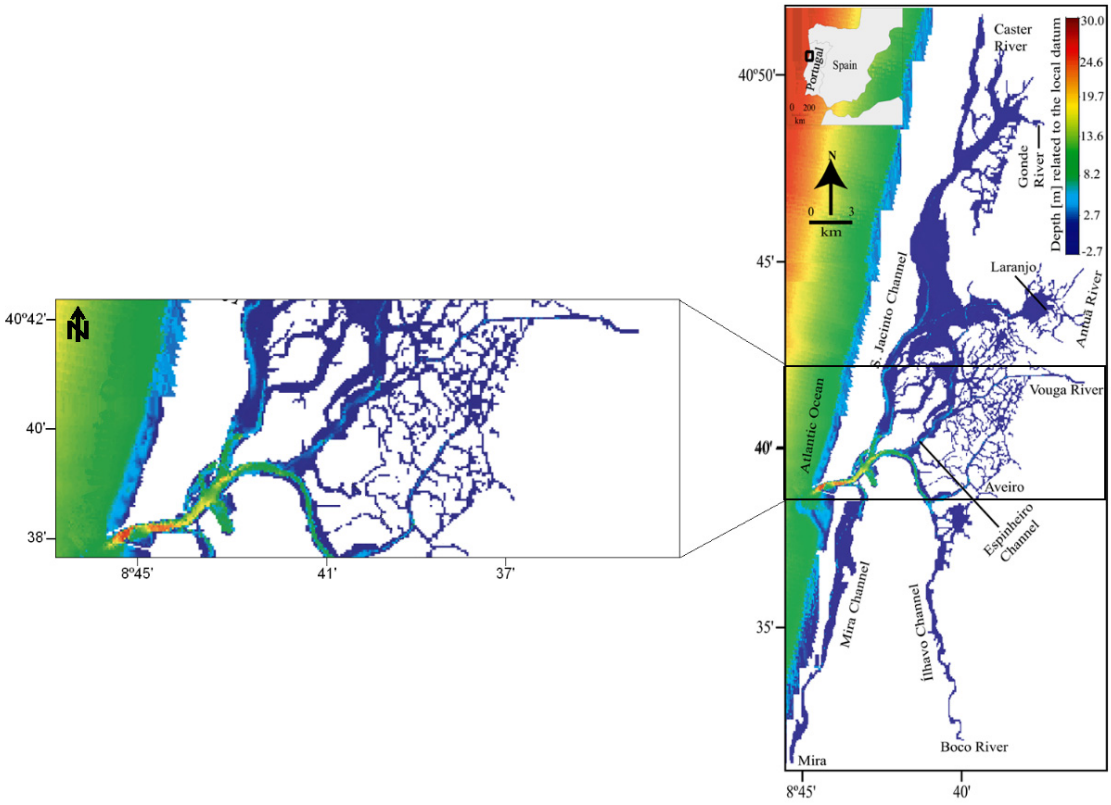

Figure 2.1: The Ria Aveiro lagoon and an enlargement of the Espinheiro channel.

3 Materials and Methods

3.1 Data

The data used in this study are: the water temperature measured in 18 sensors along the channel, the water flow between the lagoon and the ocean, the meteorological data at the University of Aveiro, the sea surface elevation (SSE) at the mouth of the lagoon and the sea surface temperature (SST) along the Portuguese coast.

The water temperature was measured through an optical sensing cable integrating fibre Bragg grating sensors. This cable is fixed along the channel bed, from the lagoon inlet to the river mouth, and is connected to a datalogger and to a GSM system. It has 18 sensors (separated by 500 m) along the 10 km allowing the long term and real time monitoring of this channel with an excellent spatial resolution. The original data have ~18 minutes of temporal resolution, and the measurements were performed sequentially from sensor 1 to 18, and therefore are not simultaneous. The field data used in this study results of 1-year measurements of water temperature data (from September 2004 to October 2005, when Portugal was under a severe drought). The data under analysis consists of 18 annual time series of water temperature with 402 days length from sampling locations 500 m distant. The original data was hourly interpolated in order to obtain simultaneously results for all sensors.

It must be noted that in Figure 3.1 and Figure 3.2, 19 sensors are represented, but sensor 16 is inactive. Sensor 1 is located near the mouth of the lagoon and the last one (sensor 19) is located near the channel's head, close to the mouth of the Vouga River. These sensors were used as a reference to the Atlantic Ocean and to the Vouga River.

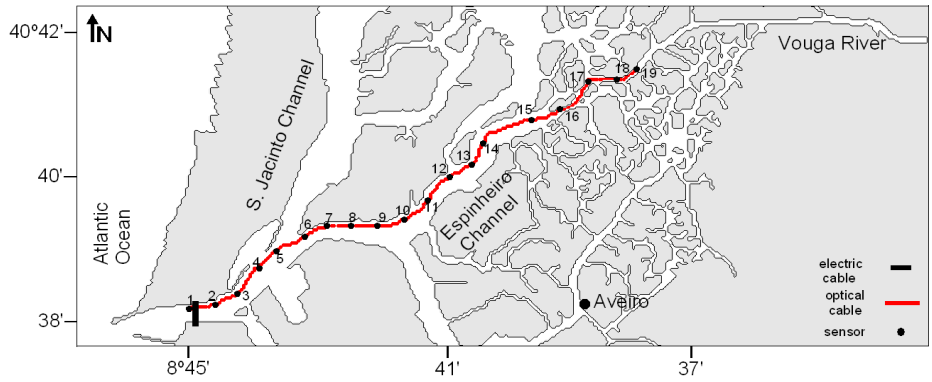

Figure 3.1: The Espinheiro channel and the location of the electrical and optical cables.

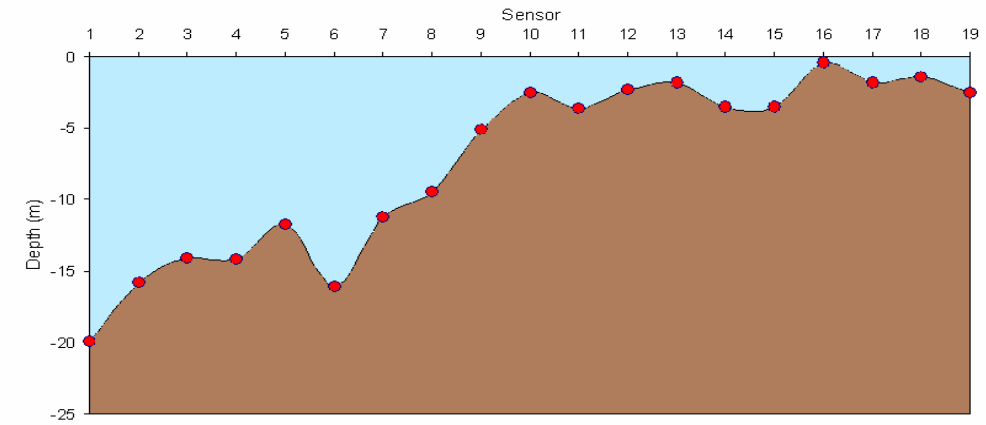

Figure 3.2: Depth at each sensor's position.

The water flow between the ocean and the lagoon was measured with an electrical cable with electrodes at its terminals deployed transversally to the inlet channel (Figure 3.3). These electrodes measure the electrical potential difference between the mouth and border of Ria de Aveiro (Figure 3.1). This electrical potential difference is induced by the effect of the geomagnetic field through charge in solitary movement with the water that flows through the channel. Then, knowing the geomagnetic field and the electrical potential difference, the water flow through the mouth of Ria de Aveiro can be quantified, allowing the study of the lagoon-ocean exchanges. This system was previously calibrated, adjusting its results with values obtained by hydrodynamic modeling. The implementation and basis of this system is fully described in Nolasco *et al*. (2006). These data are used to characterize the entrance and exit of water in Ria de Aveiro.

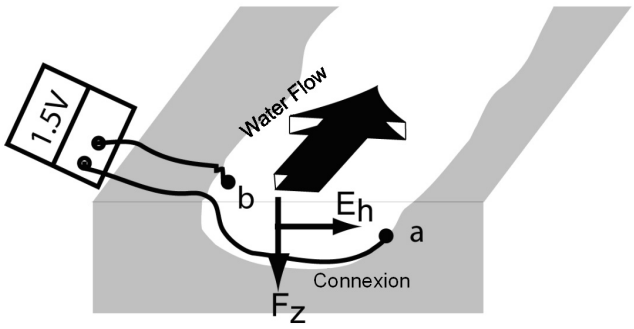

Figure 3.3: Schematic representation of the mouth of Ria de Aveiro and the electrodes placed in the northern and southern borders for the measurement of the electrical potential difference (Dias *et al*., 2003).

Hourly meteorological data (air temperature, precipitation and wind velocity) were measured at the meteorological station located at the University of Aveiro (40º38'N, 8º39'W). This data set is from October 2004 to October 2005, covering the period under analysis.

The measurements of SSE were obtained from a tidal gauge located at the mouth of the lagoon.

The satellite data were obtained from MODIS (Moderate Resolution Imaging Spectroradiometer), a key instrument aboard the Terra (EOS AM) and Aqua (EOS PM) satellites. Terra's orbit around the Earth is timed so that it passes from north to south across the equator in the morning, while Aqua passes south to north over the equator in the afternoon. Terra MODIS and Aqua MODIS are viewing the entire Earth's surface every 1 to 2 days, acquiring data in 36 spectral bands, between 0.405 and 14.385 μm, and they acquire data in three spatial resolutions: 250 m, 500 m and 1000 m. These observations can be processed to show many properties of the Earth's surface, from temperature and phytoplankton measurements near the surface of the ocean to fire occurrences and land cover characteristics on the land surface. The measurements can only be taken in ocean regions that are free of clouds and sun glint. These data were used to produce SST daily maps for the Summer months. These SST data are concurrent with the period of the water temperature data (measured by the sensors), in order to observe the influence of the SST in the water temperature measured at the sensors located near the mouth of the lagoon.

The duration of the data time series are summarized in Figure 3.4.

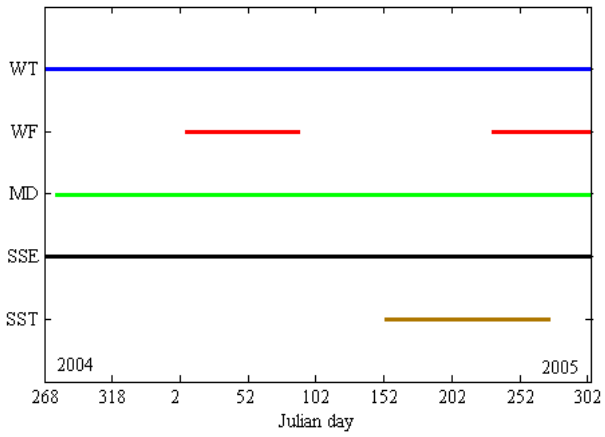

Figure 3.4: Duration of the data time series (WT-water temperature; WF-water flow; MD-meteorological data; SSE –sea surface elevation; SST-sea surface temperature).

3.2 Data analysis

Data were analyzed in order to study the spatial and temporal water temperature variability in the Espinheiro channel and its relation with the forcing mechanisms.

In order to study the spatial variability, it was necessary to proceed to a previous statistical analysis, in order to verify the behavior of water temperature along the channel. With the purpose of establishing the relevance of each tidal constituent along the Espinheiro channel, the classical harmonic analysis was applied to the water temperature data using the T_TIDE package (Pawlowicz *et al*., 2002).

The next step is the study of the water temperature temporal variability along the Espinheiro channel, evaluating the relations between the temperature data and the available meteorological and tide data along the channel. In order to separate the high frequency signal (tidal oscillations) and the low frequency signal (subtidal oscillations), the trend of the water temperature time series was removed and the series were high/low-pass filtered, considering a cut-off frequency of 0.0000093 Hz (30 h).

Spectral analysis in the domain of frequency in this work is very important because it allows the evaluation of the ocean-atmosphere interaction. These results permit to understand the impact of atmospheric perturbations and the tide over the water temperature. This analysis (8 Hanning windows) consists in partitioning the variance of a time series into a function of frequency. The study of the energy spectrum provides an alternative way of estimating the attenuation of the tidal and subtidal signals in different frequencies while progressing landwards. Spectral density plots were constructed using the *spectrum* function of MATLAB on hourly data to determine the power spectrum. Here, power is defined as energy per unit time.

Cross-spectral analysis was applied to two pairs of time series: water temperature and water level, as well as water temperature and air temperature. Before the calculations were made both high and low-pass filters were applied to all time series. The cross-spectral analysis (8 Hanning windows) provides: a co-spectrum (real part of the spectrum), which defines the relationship between the two variables (if these variables are completely independent the spectrum is zero, and if they are identical it becomes the ordinary power spectrum); a coherence spectrum, which indicates how well correlated the two sequences are as a function of frequency and a phase spectrum, which quantifies the data time lag.

Empirical Orthogonal Function (EOF) analysis provides a convenient method for studying the spatial and temporal variability of long time series of the water temperature data over large areas. Among the various available methods of analysis, this one is a particularly useful tool to study large quantities of multi-variate data.

EOF analysis divides the temporal variance of the data into orthogonal spatial patterns called empirical eigenvectors and establishes spatial patterns of variability. Moreover it is computed the associated time variation to each EOF and also assigned a value of "importance" to each pattern (Bjornsson and Venegas, 1997). In other words, EOF analysis is used to decompose a time-series into its orthogonal component modes, the first few of which can be used to describe the dominant patterns of variance in the time series. The lowest modes have the largest spatial scales and represent the most dominant modes of variability. This method is fully described in Emery and Thompson (1997).

In order to established the relation between the temporal variation of the water temperature inside the channel and the inter-annual variability of the air temperature, the correlation between the first principal component (PC1) of the first EOF and the air temperature was calculated.

Finally, correlations between the water temperature measured in the sensors and the forcing variables (tide, air temperature, sea surface temperature) were also calculated.

4 Observations and environmental data

4.1 Meteorological conditions

In Figure 4.1 are plotted the hourly values of air temperature and precipitation and daily values of wind velocity measured at the Aveiro meteorological station from October 2004 to October 2005.

The annual average temperature during this period is 15.3 ºC; the average temperature for Winter months is 9.3 ºC, and for Summer months is 20.2 ºC. In the last months of the study period the air temperature reaches unusual high values, such as 35.5 ºC in the beginning of June 2005 and 38.2 ºC in the mid-July 2005.

The rainy season was the Autumn of 2004, reaching a daily maximum of about 58 mm. During the other seasons almost there was no precipitation in this zone (severe drought). The only exception was in March where some rainfall existed. According to Fonseca *et al*. (1988) the annual average precipitation in Aveiro region is 913.5 mm. Since there was almost no precipitation during the study period, the river flow was considerably lower than the typical values.

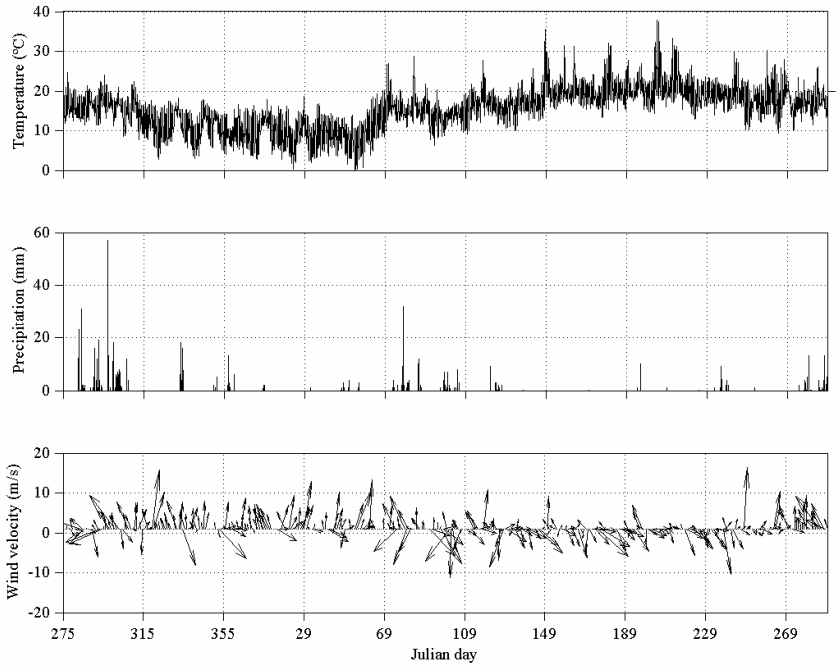

Figure 4.1: Air temperature, precipitation and wind velocity in Aveiro meteorological station, from October 2004 to October 2005.

The wind velocity maximum was found in the beginning of Winter and in the beginning of Autumn, reaching a daily maximum of 15 and 18 ms^{-1}. The mean values of wind velocity remain almost constant during all year with values around 3.7 ms^{-1}. Figure 4.1 also shows high frequency of winds blowing from North and Northwest directions. These northern winds are characteristic of the Summer season. In the Winter the wind regime is more variable, with strong fluctuations in direction and intensity, with predominance winds blowing from South and Southwest.

4.2 Tides

Figure 4.2 shows (as example) the time series for a 26-day period of hourly values of the water level.

The tide was semi-diurnal with a diurnal inequality. A minimum water level of 0.6 m and a maximum water level of 3.3 m in the spring tide have been observed. The minimum tidal amplitude during this period was 1.3 m at neap tide and the maximum amplitude at spring tide was 2.65 m.

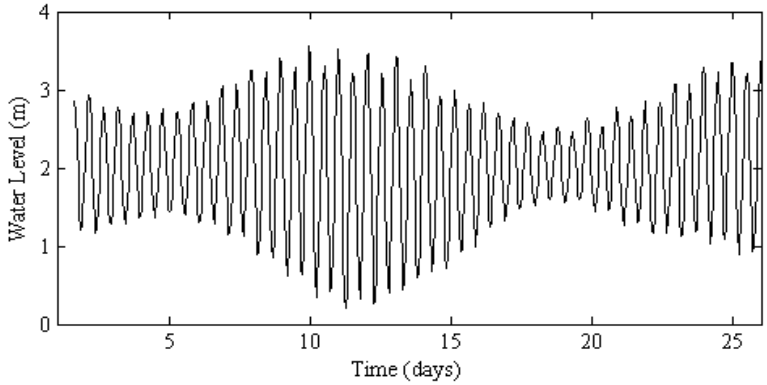

Figure 4.2: Time series of the water level. Hourly records (1 to 26 February 2005).

4.3 Water flow

Figure 4.3 shows the tidal lunar water flow determined using measurements of electrical potential difference in mouth of the Ria de Aveiro for the complete data set (Figure 4.3a) and 26-day period (Figure 4.3b).

The water flow has a similar behavior to the tide (as expected). These data are used only to characterize the water exchange between the Ria de Aveiro and the near ocean. The

water transport during the flooding is responsible for the ocean water entrance into the estuary.

The average values of total flow through the inlet during flood and ebb for spring and neap tide were computed (Figure 4.3b). During spring tide, the average value of water flow passing across the bar during the flood period is 4239.1 m^3s^{-1} and during the ebb period is 4260.4 m^3s^{-1}. During neap tide, the average value during flood is 2540.2 m^3s^{-1} and during the ebb is 2813.3 m^3s^{-1}. From these results it may be concluded that during this period the water exchange is greater in the ebb. The highest values of water flow are found in spring tide, and the lowest in neap tide, reinforcing the importance of the fortnight modulation in Ria de Aveiro.

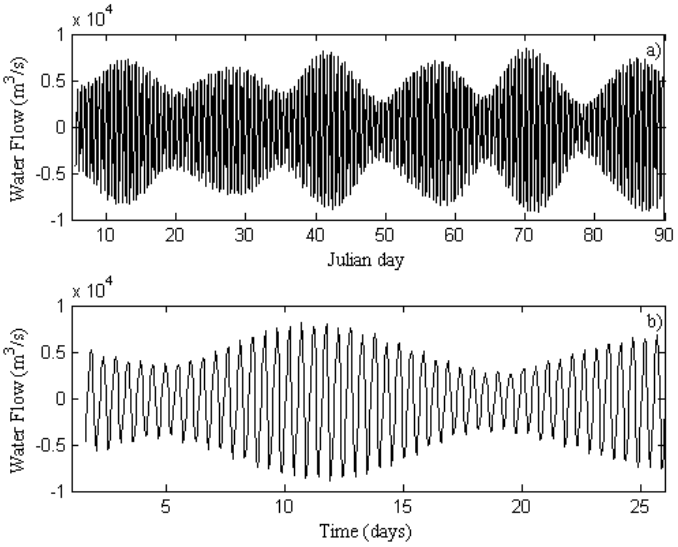

Figure 4.3: Tidal lunar water flow in mouth of the Ria de Aveiro. a) Records obtained between 6 January and 30 March 2005; b) Records obtained between 1 and 26 February 2005.

5 Results and Discussion

5.1 Spatial variability

Figure 5.1 shows the average water temperature distribution along the Espinheiro channel. These figures are obtained by monthly-averaging the water temperature data from each sensor. The field data for sensor 16 (7.5 km) does not exist, as previously referred.

In general, it can be observed that the water temperature values decay from Autumn to Winter. During the Winter months, water temperature is nearly constant along the channel, but slightly decreasing towards the channel's head (the oceanic water temperature is usually higher than the freshwater temperature). In Summer, the water temperature distribution along the channel follows the same pattern. Two minima (12-14 ºC) in positions 2.5 and 3.5 km and one maximum (18-20 ºC) at 5.5 km from the mouth are observed.

In the mouth of the channel, the water temperature ranges from 14 ºC during Winter to 17/18 ºC during the Summer. Near the channel's head, which is the fluvial region, the water temperature ranges from 12 ºC during Winter to 16/17 ºC during Summer. The measurements show that the water temperature values in the mouth during Summer months are higher than those measured in the channel's head, revealing a tendency opposed to what would be expectable. This fact may be explained by a river flow lower than the typical values during the study period.

The difference between the inlet ocean temperature and the temperature at the far end of the channel can reach 2 ºC (in Winter season), these spatial differences being important in the net export of heat energy from the lagoon toward offshore waters.

For the entire survey period, the water temperature between positions 2.5 and 3.5 km is the lowest. This fact may be explained by the sensors location in the São Jacinto and Espinheiro channels convergence, where on ebb the water temperature could be lower, as it was recorded in these sensors (the water that leaves the São Jacinto channel could be colder than the water that comes from the upstream area of the Espinheiro channel). This may also be due to some technical problems affecting these sensors.

Between positions 5.5 and 6.5 km the water temperature presents its maximum values during Spring and Summer (about 20 ºC). This may be explained by the channel's

shallowness, and by the key role of the meteorological variables like air temperature and solar radiation in the water heating/cooling cycle.

The water temperature distribution is less dependent on the river discharge and it is closely related to the inter-annual air temperature variation (Figure 4.1). As, in the study period the river flow was quasi null. Therefore this forcing should be considered of minor importance in the characterization of the longitudinal water temperature distribution during the study period.

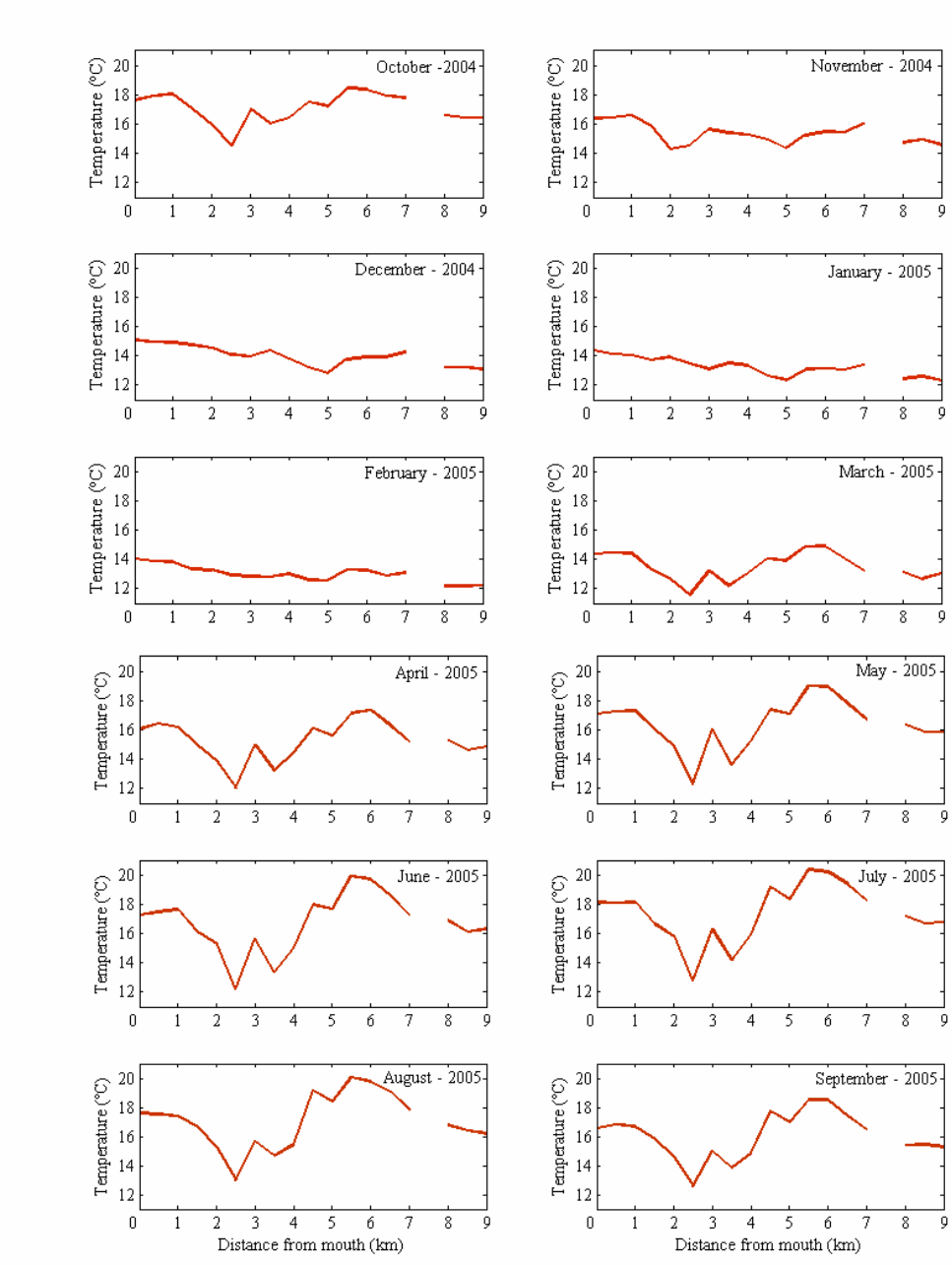

Figure 5.1: Mean water temperature along the Espinheiro channel.

5.1.1 Harmonic analysis

The importance of each tidal constituent on the water temperature distribution along the Espinheiro channel can be evaluated through the application of the classical harmonic analysis (Pawlowicz *et al*., 2002) to the data. The results for six major tidal constituents (K_1-23.93 h (principal solar); S_1-24 h (radiational); P_1-24.07 h (principal solar); S_2-12 h (principal solar); T_2-12.02 h (larger elliptical solar); M_2-12.42 h (principal lunar)), are plotted in Figure 5.2.

Through the analysis of Figure 5.2a, it can be observed that the major tidal constituent is S_1 (about 1.4 ºC of amplitude along the channel), revealing the diurnal periodicity and the importance of the meteorological variables (air temperature, relative humidity, cloud cover and solar radiation) on the water heating/cooling cycle. S_2 is the constituent that follows in amplitude (about 0.3 ºC) but only in some parts of the channel, specifically between positions 1-5 km and 8-9 km. In positions 0.5, 5.5, 6 and 8.5 km M_2 is the highest (about 0.4 ºC), as expected, since M_2 has most of the tidal energy in Ria de Aveiro and for this reason can be considered representative of the tide in this lagoon (Dias *et al*., 1999).

The other constituents, such as T_2, P_1 and K_1, have similar amplitudes (about 0.15 ºC along the channel).

In Figure 5.2b, it can be observed that the phase of the harmonic constituents increase along the channel. The water temperature propagation along the channel is altered by the channel bathymetry. A change in the estuarine bathymetry will most often alter the circulation within an estuary (Harcourt-Baldwin and Diedericks, 2006).

Between positions 5.5 and 6.5 km the phase is about 92º (almost 6.3 hours) for the S_1 constituent and about 350º (almost 12.1 hours) for the M_2 constituent. In these positions, there is a rapid phase change due to an increase in the friction (a shallow area). More specifically, the phase of the diurnal constituents decreases and the phase of the semidiurnal ones increases. This may be due to the fact the phases of harmonic constituents are mainly affected by friction while their amplitudes are both damped by friction and amplified or eventually diminished by the geometry along the channel (Hsu *et al*., 1999).

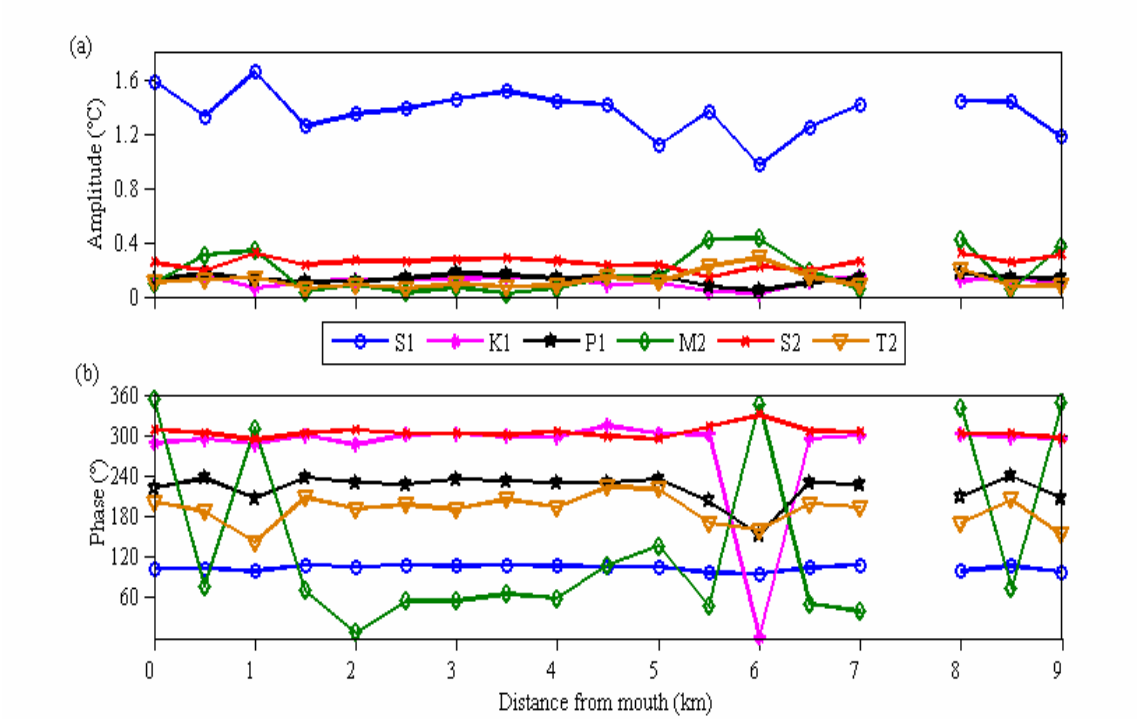

Figure 5.2: Distribution of tidal amplitude (a) and phase (b) for S_1, K_1, P_1, M_2, S_2 and T_2 along the Espinheiro channel.

5.2 Temporal variability

In this section the temporal variability along the Espinheiro channel is studied and for reasons of simplification, the following steps of this work will not include results for all sensors. The selection was made taking into account the sensors location and general contribution to the comprehension of the system and so only the sensors that exhibited more important characteristics for the study were selected. The selected studied sites were: sensor 1, located near the Barra of Aveiro, which is of interest to the study because it measures water characteristics very similar to seawater; sensor 2, located between the tide-gauge and Triângulo das Marés; sensor 6, located in the beginning of the São Jacinto channel; sensor 10, located at beginning of the Ílhavo channel, which is interesting to understand the importance of the water exchange between the Espinheiro channel and the adjacent channels; sensor 13, located in a shallow area and where the temperature recorded by the sensors is higher; finally, sensor 19, which presents a location near the mouth of the Vouga River, whose contribution as a main source of freshwater into the Espinheiro channel is generally non- negligible.

With the purpose of analyzing the results as a function of frequency, they were decomposed into high and low frequencies, using the filter referred on Section 3.2. The influence of the meteorological forcing in the time series is recognizable through the application of a low-pass filter (subtidal frequencies), while the high-pass filter shows evidence of tidal forcing (tidal frequencies).

From Figure 5.3 to Figure 5.8 both the original and filtered time series of the water temperature measured in sensors 1, 2, 6, 10, 13 and 19 are represented.

In general, all sensors measure similar temperature variations throughout the year. There is evidence of seasonal variation, as the water temperature is lower in Winter and higher in Summer, which is observed in all sensors. This seasonal variation is mainly observed at the low frequencies, and it dictates the behavior of the time series in terms of long term general variability. The high frequencies, on the contrary, are responsible for the daily variation and do not contribute to the global pattern of variation. The water temperature measured by sensor 6 has a quasi-constant pattern during the whole year.

In the subtidal frequencies, a similar pattern can be observed for all sensors (with the exception of sensor 6), which revealed a general trend for water heating during the Summer months and for water cooling during the Winter months. Consequently, the water temperature can vary ± 5 ºC due to the long term processes, which can be attributed to the warming/cooling global effects inherent to the dynamics of the planet throughout the seasons. In the tidal frequencies, the solar heating effect can clearly be observed, reinforced by the semidiurnal and diurnal effect the tidal origin.

At the subtidal frequencies, the pattern obtained for Ria de Aveiro is dictated by weather and/or meteorological long term events. The increase of the subtidal oscillations is greater in Winter than in Summer, which is likely to be related to sudden changes in the meteorological conditions over the area, shown in the abrupt changes in wind direction in Figure 4.1. The low frequencies and the wind velocity have similar patterns. Strong winds resulted in changes in the water temperature. Depending on the direction, they will either cause a decrease if blowing southwards or an increase if blowing northwards (e.g. on Julian day 320 (15 November) the wind velocity was 18 ms^{-1} and the water temperature diminishes by 1 ºC). Harcourt-Baldwin and Diedericks (2006) showed that the wind has a strong influence on the formation of a density current in Tomales Bay. In the lower

Chesapeake Bay, Paraso and Valle-Levinson (1996) found that the wind forcing were responsible for the horizontal water temperature gradient.

Observing in more detail, in Figure 5.3a and Figure 5.4a the behavior of the water temperature is similar, what may be explained by the very short distance between these sensors. The mean of the water temperature measured in these sensors is about 16 ºC. The water temperature measured in these sensors is mainly influenced by the tide and the oceanic water temperature (due to the proximity of the sea). The temperature at the entrance of the mouth exhibits strong tidal fluctuations and a diurnal inequality.

In Figure 5.5a, the water temperature is low (about 13 ºC) independently of the season for the whole study period. As previously mentioned, it may be due to the sensors location in the São Jacinto and Espinheiro channels convergence. However, there is evidence of two maxima around Julian days 259 (16 September) and 299 (26 October) of 17.9 ºC and 18.7 ºC, respectively. The first maximum is observed in the low frequencies (3 ºC) (Figure 5.5c); this may be due to the occurrence of a strong change in the wind direction, as can be observed in Figure 4.1, where the wind changes from southward to northward. This maximum is observed in all time series. The second maximum is observed in the high frequencies (5.6 ºC).

The water temperature measured in sensor 13 (Figure 5.7a), located about 1.5 km of sensor 10 (Figure 5.6a), presents a similar behavior (the mean of the water temperature is about 16.5 ºC), probably due to the higher air temperatures and the shallowness of these sensors location (a decrease in depth resulted in warmer water temperatures) (Figure 3.2). The maximum temperatures measured in these sensors are reached at the far end of the channel, where the tidal effect is not so strong. The mean of the water temperature measured in sensor 19 (Figure 5.8a) is 14.8 ºC. The decrease of the water temperature in this sensor may be explained, by its location near the mouth of the Vouga River. Although the river flow was reduced, it can have some influence on the water temperature.

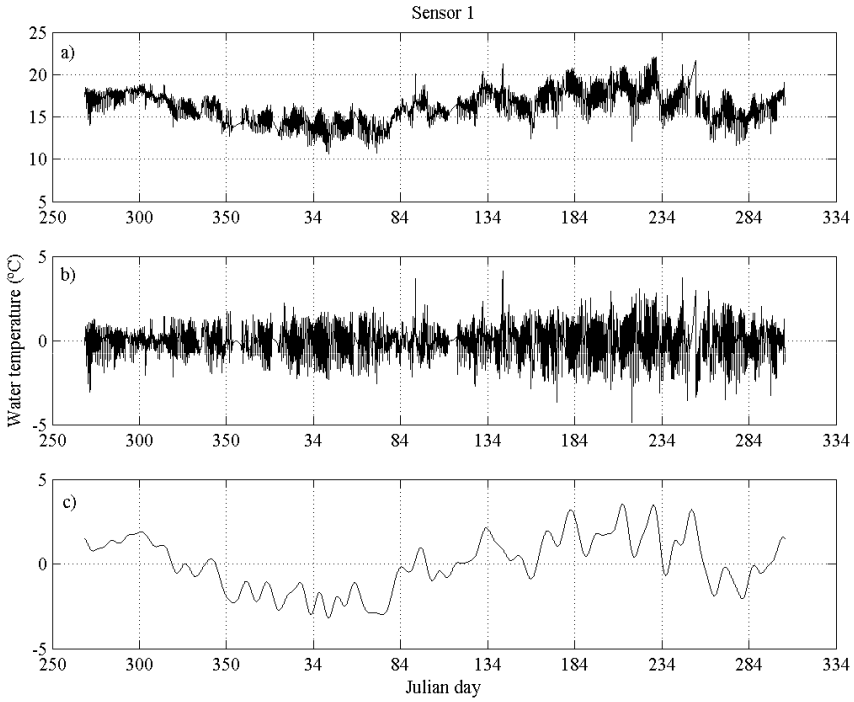

Figure 5.3: Original (a) and filtered time series of the water temperature measured in sensor 1, showing the high (b) and low frequencies (c).

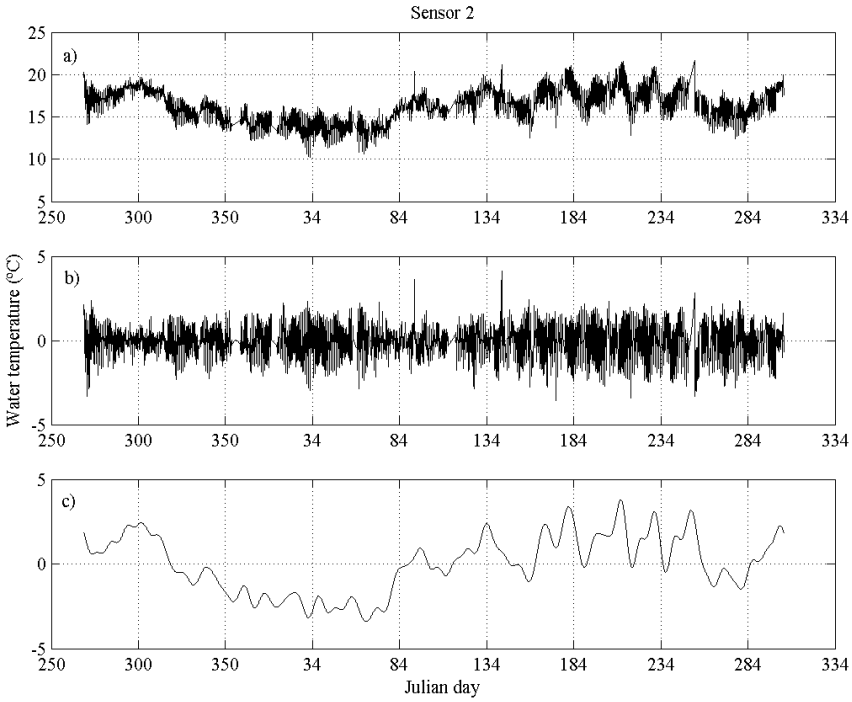

Figure 5.4: Original (a) and filtered time series of the water temperature measured in sensor 2, showing the high (b) and low frequencies (c).

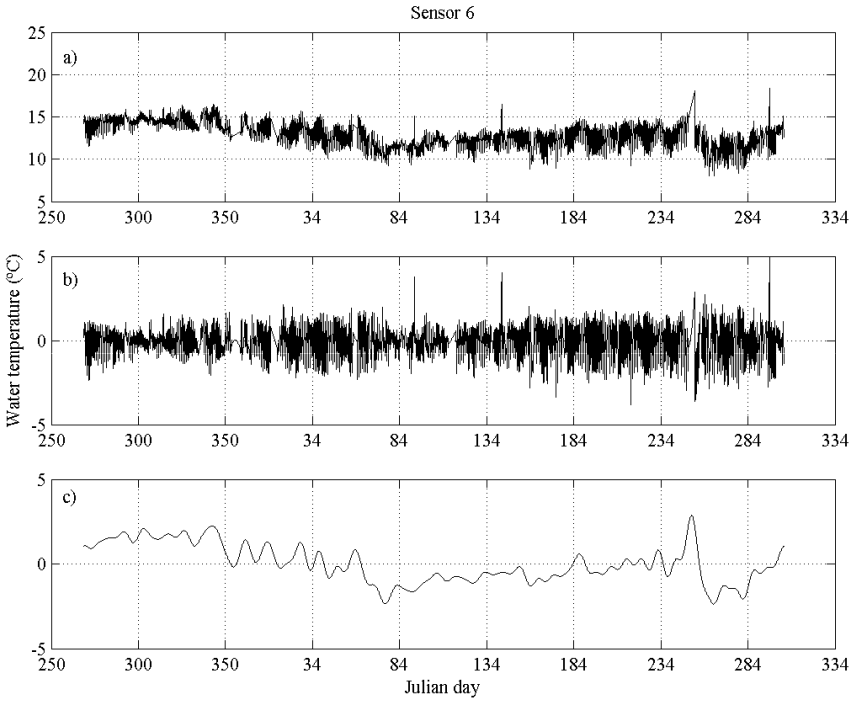

Figure 5.5: Original (a) and filtered time series of the water temperature measured in sensor 6, showing the high (b) and low frequencies (c).

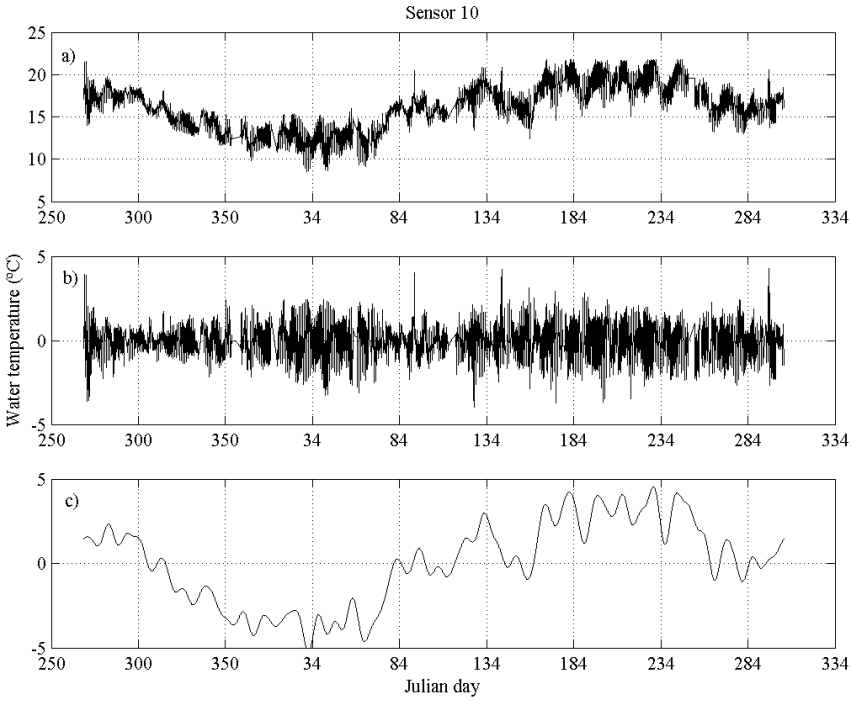

Figure 5.6: Original (a) and filtered time series of the water temperature measured in sensor 10, showing the high (b) and low frequencies (c).

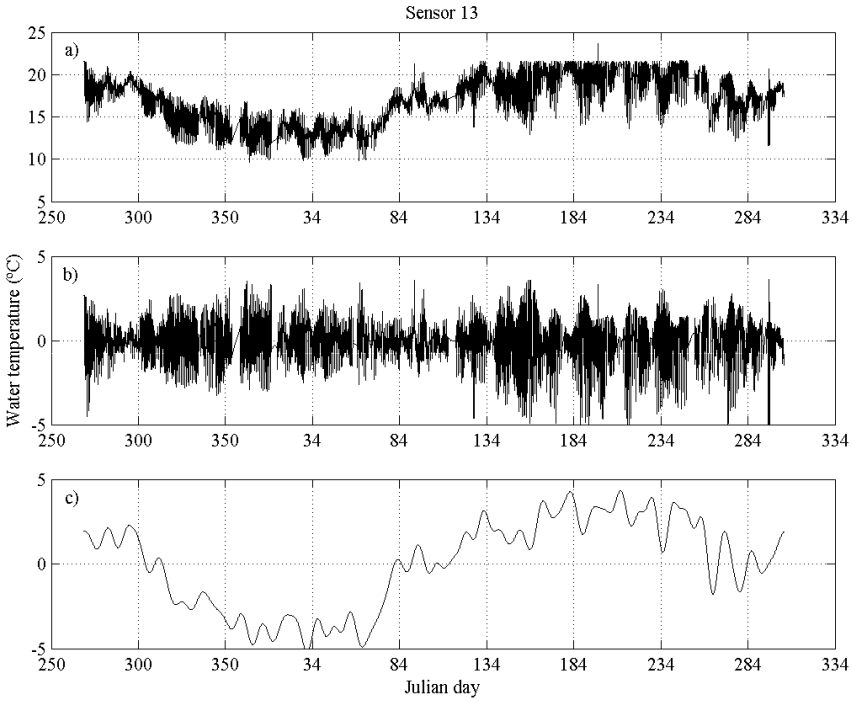

Figure 5.7: Original (a) and filtered time series of the water temperature measured in sensor 13, showing the high (b) and low frequencies (c).

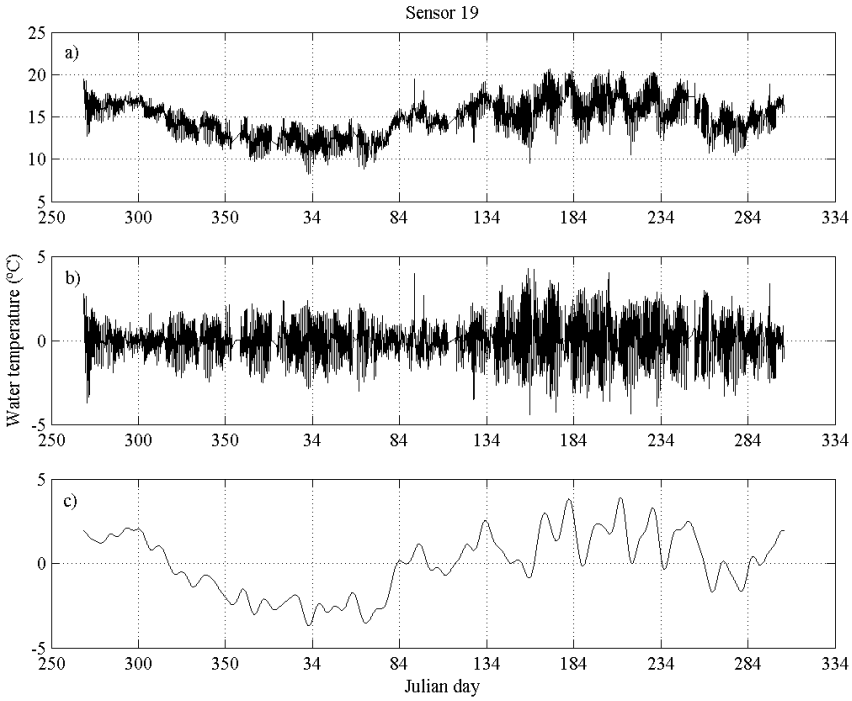

Figure 5.8: Original (a) and filtered time series of the water temperature measured in sensor 19, showing the high (b) and low frequencies (c).

5.2.1 Spectral analysis

Spectral density plots were used to determine the power spectrum and to find any periodic phenomena. Before performing the spectral analysis, the time series trend and mean was removed. Energy spectral density plots of the water temperature measured in sensors 1, 2, 6, 10, 13 and 19 are depicted in Figure 5.9.

The most energetic peaks are found at the diurnal and semidiurnal frequencies, but contributions at tridiurnal and quarterdiurnal tidal frequencies were also found. The energy spectrum also presents energetic subtidal oscillations (LP). Results also indicate that subtidal processes are usually less energetic than the diurnal oscillations, except in situations of extreme events, when the subtidal frequencies are amplified along the channel. Subtidal processes are more energetic than semidiurnal and quarterdiurnal oscillations and have frequencies varying from 3 to 23 days.

In all sensors spectra, two main peaks are observed: one diurnal and one semidiurnal. The diurnal peak is the most energetic (almost 10 times higher) (in sensors 1, 2, 6, 10 and 19), revealing the importance of the heating solar on the heating/cooling cycle of the water. In sensor 13 spectrum, three main peaks are observed, one diurnal, one semidiurnal and one quarterdiurnal. The semidiurnal peak is the most energetic one, but with a slight difference to the diurnal peak. The semidiurnal peak is associated to the tidal main periodicity in Ria de Aveiro. The peaks corresponding to the 3 and 4 cycles/day frequency are probably originated by the non-linear interaction between the propagation of the main tidal constituents and the bottom friction, as that sensor is located in a shallow area (Figure 3.2). Concerning sensor 19, the same effect can be observed, but the diurnal peak is more energetic than the semidiurnal one (see Figure 5.2).

The diurnal peak importance in the spectrum can be explained as follows: the Ria de Aveiro is a shallow water estuarine system with mean depth of about 1 m (over the local datum), and the water temperature is conducted not only by the tide, that has an important contribute at these frequencies, but also by heating from solar radiation incidence and air temperature daily variability. The semidiurnal peak in spectrum of the water temperature is related to the water input due to the tidal wave propagation along the channel. The results of the spectral analysis confirm the harmonic analysis results (Figure 5.2).

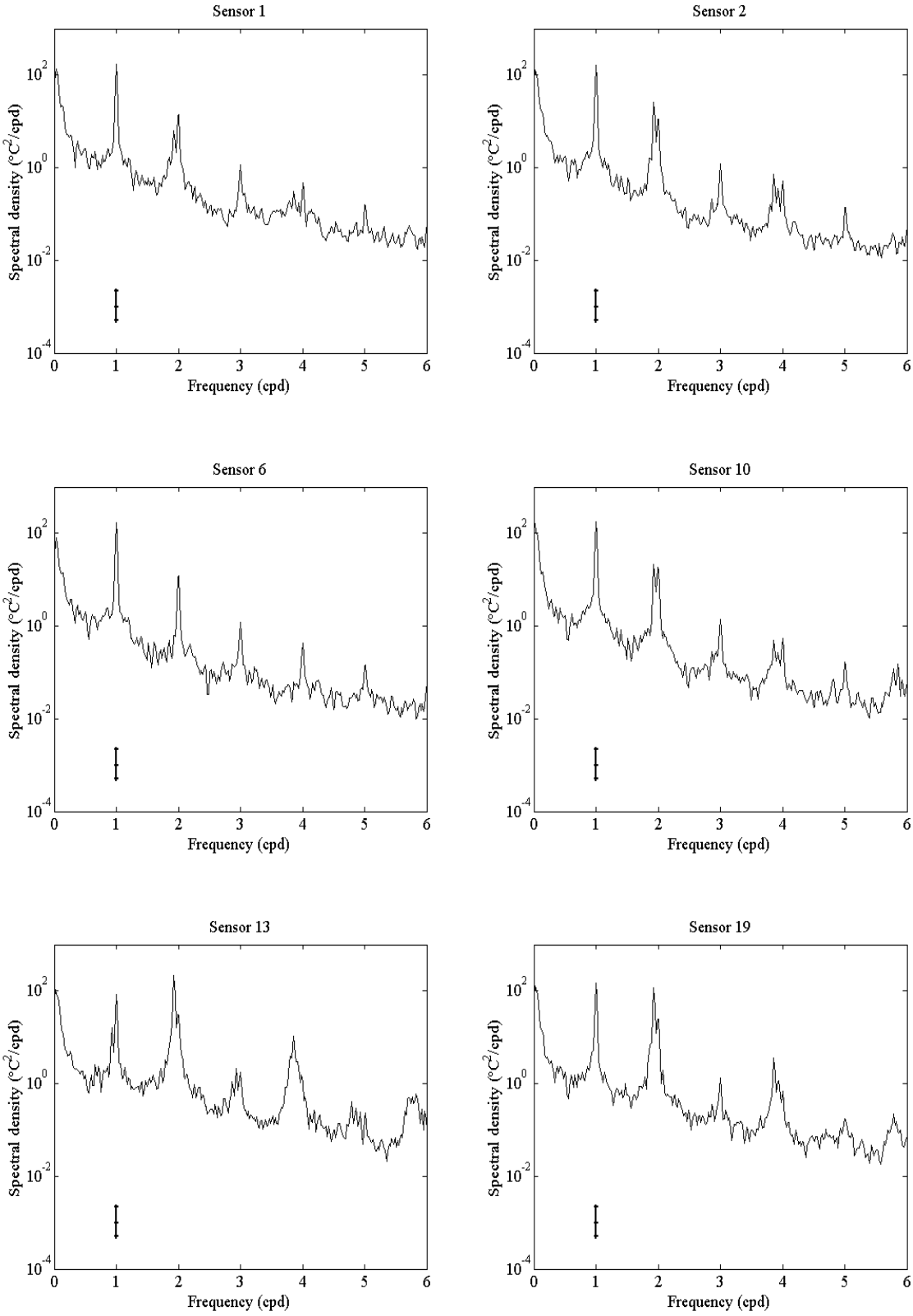

Figure 5.9: Energy spectrum of the time series of water temperature measured in sensors 1, 2, 6, 10, 13 and 19. The vertical bar indicates a 95% confidence level.

5.2.2 Cross-spectral analysis

The tides are the main forcing of the circulation in the Ria de Aveiro. In order to determinate the relationship between the water level and water temperature measured in sensors 1, 2, 6, 10 and 13, and also to obtain the phase difference and the coherence, the cross-spectral analysis was applied to the data (Figure 5.10 to Figure 5.15).

In general, through the analysis of these figures, it can be observed that the water temperature and the water level reveal more significant coherence in sensor 2.

Considering now only Figure 5.11, we can see that the water temperature and water level were coherent at frequencies between 1 (0.55) and 2 cycles/day (0.75). This highest correlation reveals that heat is transported significantly by the tide from the nearly ocean. At these frequencies the co-spectral density function indicates that the oscillations of the water level are well correlated, in particular at the semidiurnal frequencies (due to the proximity of the sea). For this semidiurnal period, the phase lag obtained between the two parameters is 2.54º, which corresponds to 5.5 minutes. The minimum of the water temperature measured in sensor 2 has a phase lag of 5.5 minutes, relative to the high tide in Barra.

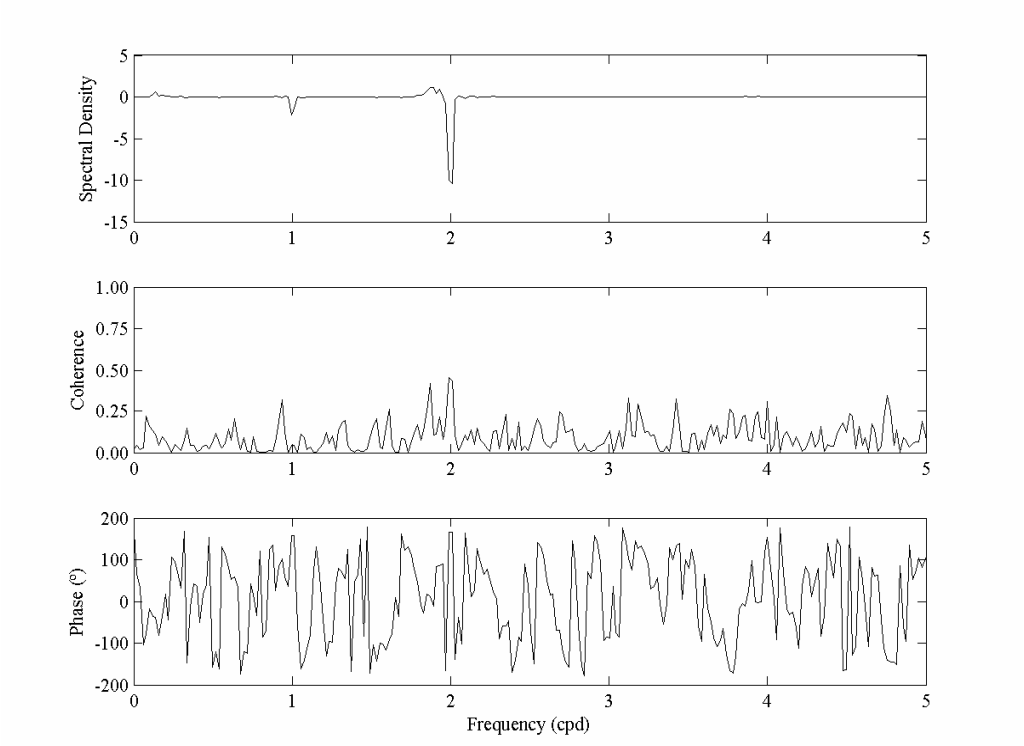

Figure 5.10: Cross spectrum, coherence and phase between the water level in Barra and the water temperature measured in the sensor 1.

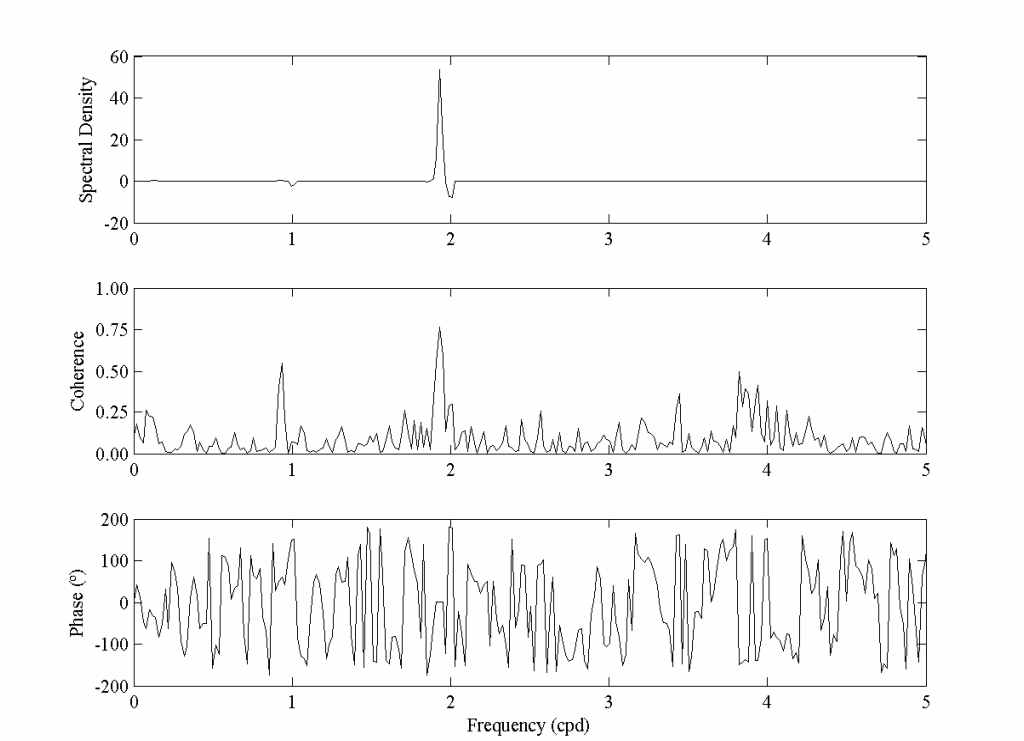

Figure 5.11: Cross spectrum, coherence and phase between the water level in Barra and the water temperature measured in the sensor 2.

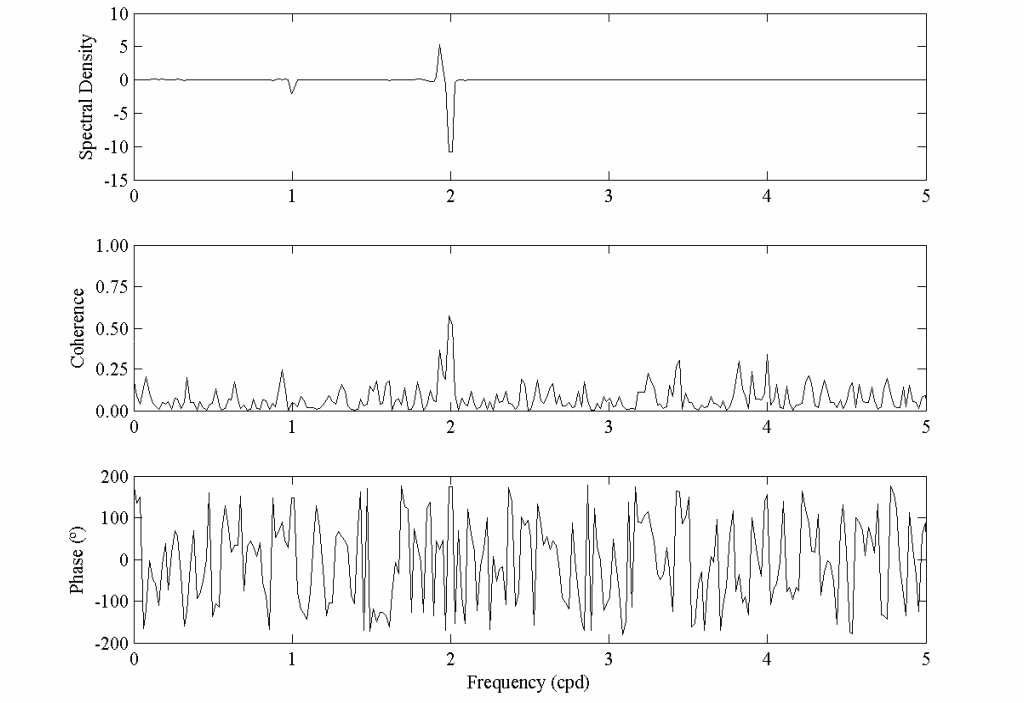

Figure 5.12: Cross spectrum, coherence and phase between the water level in Barra and the water temperature measured in the sensor 6.

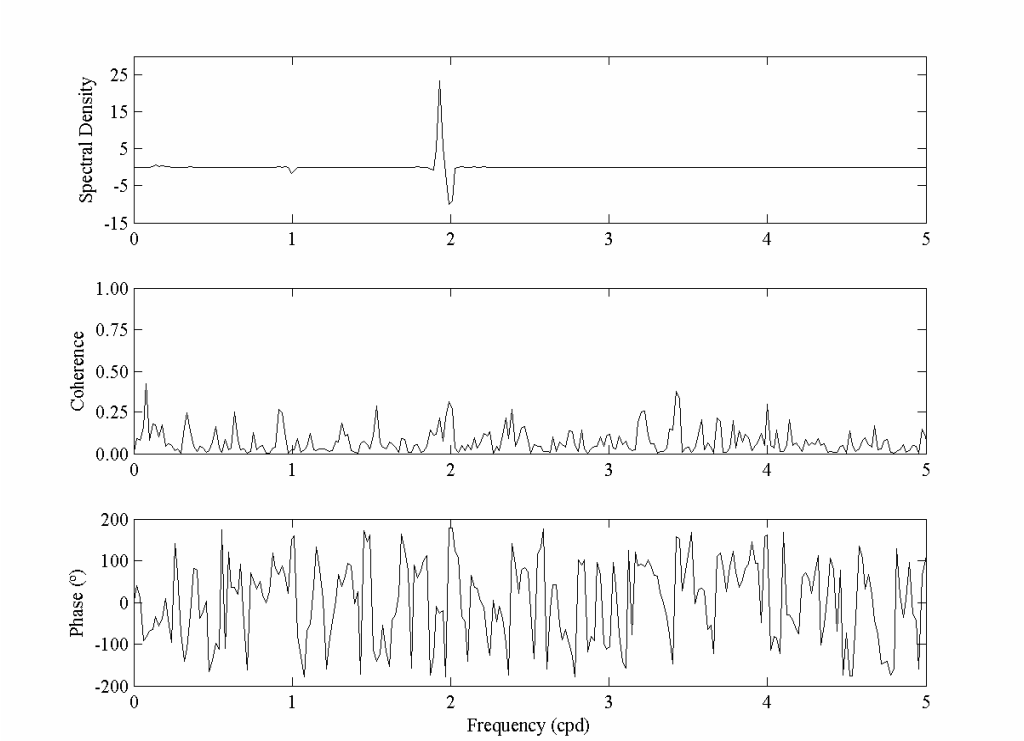

Figure 5.13: Cross spectrum, coherence and phase between the water level in Barra and the water temperature measured in the sensor 10.

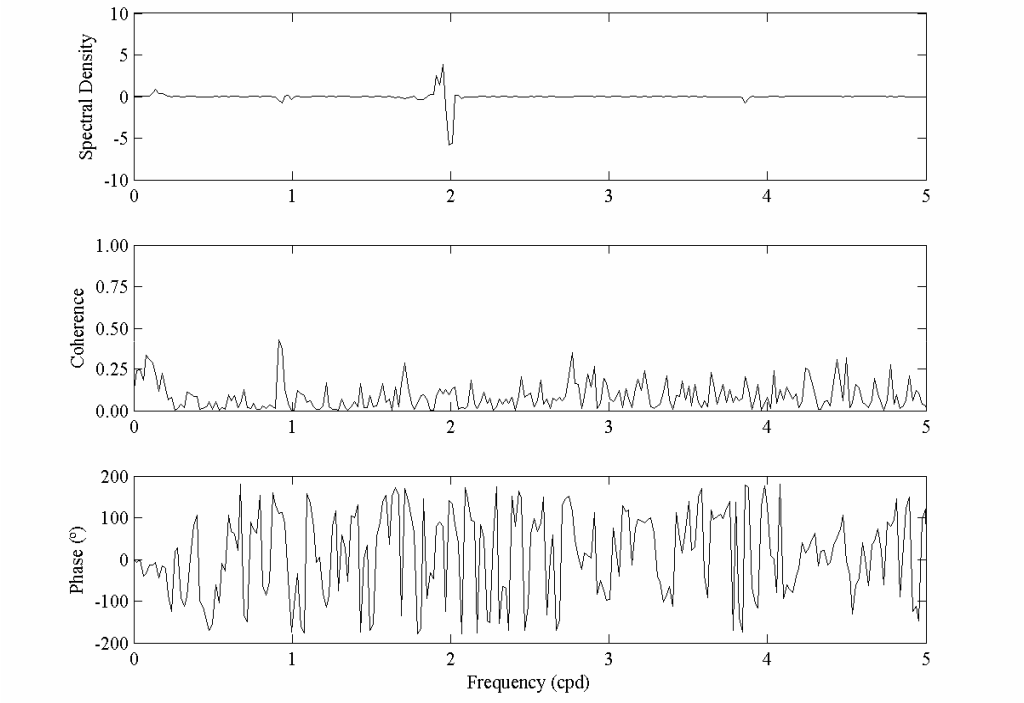

Figure 5.14: Cross spectrum, coherence and phase between the water level in Barra and the water temperature measured in the sensor 13.

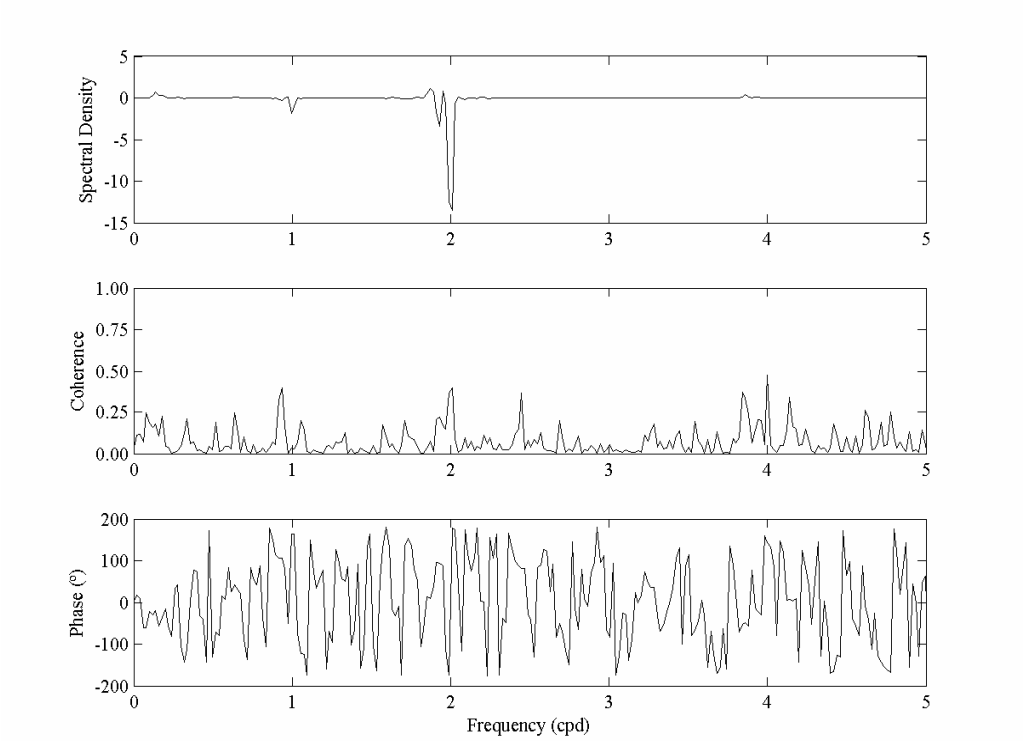

Figure 5.15: Cross spectrum, coherence and phase between the water level in Barra and the water temperature measured in the sensor 19.

In Figure 5.12 it can be observed that in semidiurnal frequencies, the co-spectrum presents negative values, which means that when the tidal range increases, the water temperature decreases.

The cross spectrum obtained between the water level in Barra and the water temperature measured in sensors 10 and 13 has not high coherence in any frequency band, as observed, indicating that the influence of the tide in these areas is small. Sensor 10 is located at the beginning of the Ílhavo channel, where the tidal prism in this channel is about 13.5% relative to the tidal prism at the mouth (Dias, 2001). The tidal effect may be attenuated whenever there is convergence of two channels. In other words, the tide is distorted as it progress from the mouth towards the end of the channels.

But at Figure 5.15 the spectra reveal the existence of energy peaks corresponding to the first harmonics of the semidiurnal constituents (coherence of about 0.5), revealing the importance of the shallow water constituents in a system like the Espinheiro channel.

Results for the cross-spectral-analysis obtained between the water level in Barra and water temperature measured in sensor 18 (not shown) shows that they were coherent (0.6)

at the semidiurnal frequencies. For this semidiurnal period, the phase lag obtained between the two parameters is 169.5º, which corresponds to 5.85 hours and the minimum of the water temperature measured in sensor 18 (8.5 km from the mouth).

Results show that the semidiurnal and diurnal frequencies are attenuated from the mouth to the far end of the channel, and that there is significant phase delay between the mouth and each sensor. Ria de Aveiro is a very shallow lagoon with a very complex geometry and for these reasons distortion occurs as the tidal wave propagates along the shallow channels.

The air temperature is an important factor in the determination of the water temperature variability. In this way it is important to evaluate the phase lag between the air temperature and the water temperature measured in the sensors distributed along the Espinheiro channel and so the cross-spectral analysis was applied to the data (Figure 5.16 to Figure 5.21).

In general, the co-spectrum, coherence and phase spectra show that the time series of air temperature and the water temperature measured in each sensor have a coherence of almost 1 at the diurnal frequencies. At this frequency the co-spectral density function indicates that the oscillations between the air temperature and the water temperature at each sensor are well correlated.

The negative values in the co-spectrum and the behavior of phase spectra show that the air temperature at the station is out of phase by approximately 180º relative to each sensor.

Results for the cross-analysis obtained between the air temperature and water temperature measured in sensor 1 (Figure 5.16), show that they are coherent (0.83) at the diurnal frequencies. For this diurnal period, the phase lag obtained between the two parameters is -145.2º, but the diurnal peak of the co-spectrum is negative (180º-145.2º), which corresponds to the 2.32 hours. In other words, 2.32 hours is the time of response of the water temperature to undergo the influence of the air temperature. It is also visible in this figure that, in the low frequency band (about 10 days), the two variables were coherent (0.5), with lower energy than the diurnal peak. The same occurs in Figure 5.18 however, the coherence decreases significantly, indicating that the influence of the prescribed low frequency oscillations in these areas is small.

Figure 5.19 shows that the water temperature measured in sensor 10 and the air temperature were coherent at the diurnal frequencies. This sensor is located in a shallow area (~ 4 m). The phase lag is -150º, which corresponds to 2 hours, while in Figure 5.20 is of -157.3º, in this case corresponding to 1.5 hours. As it can be observed, the time of response of the water temperature to undergo the influence of the air temperature decreases as it goes further into the channel (the water column height decreases) (see Figure 3.2). This means that the temperature of the estuarine water column is controlled by the solar radiation. A similar result was found by Sepúlveda *et al*. (2004) in the Rio de la Plata estuary.

In summary, the water temperature distribution along the Espinheiro channel closely followed the air temperature and was modulated by tidal variations. The solar radiation heating effect is important for the establishment of temperature patterns, especially in the sallow areas at the far end of the channel.

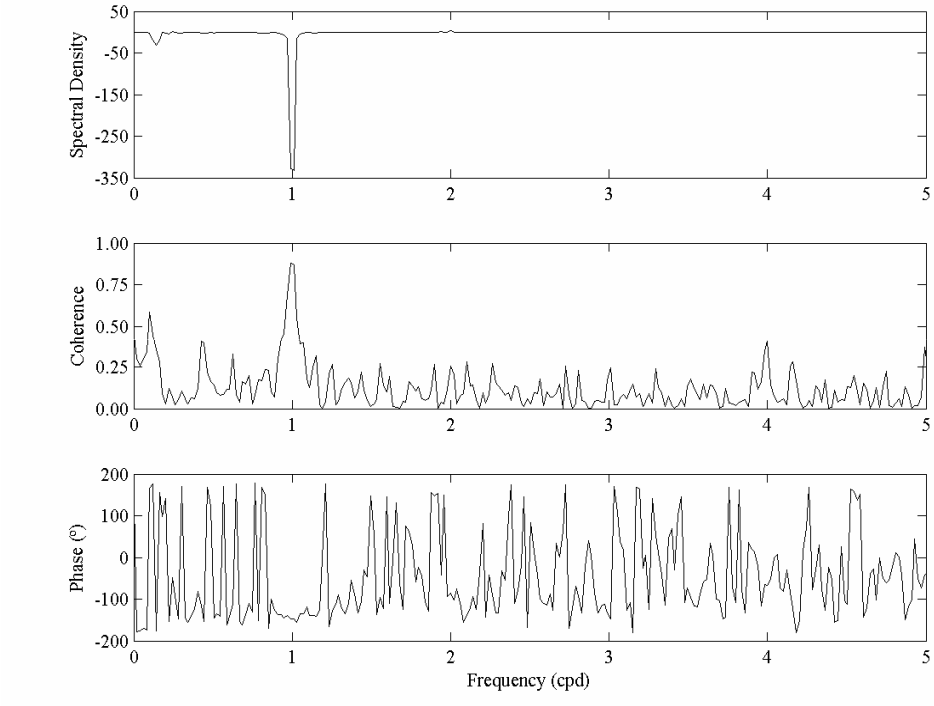

Figure 5.16: Cross spectrum, coherence and phase between the air temperature and the water temperature measured in the sensor 1.

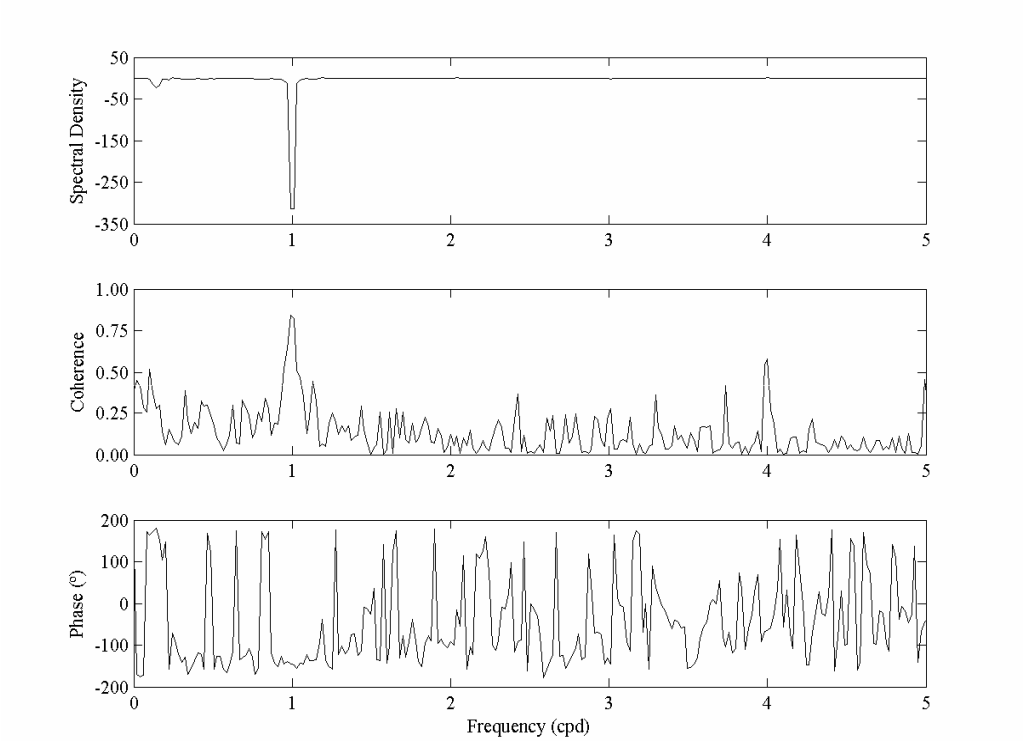

Figure 5.17: Cross spectrum, coherence and phase between the air temperature and the water temperature measured in the sensor 2.

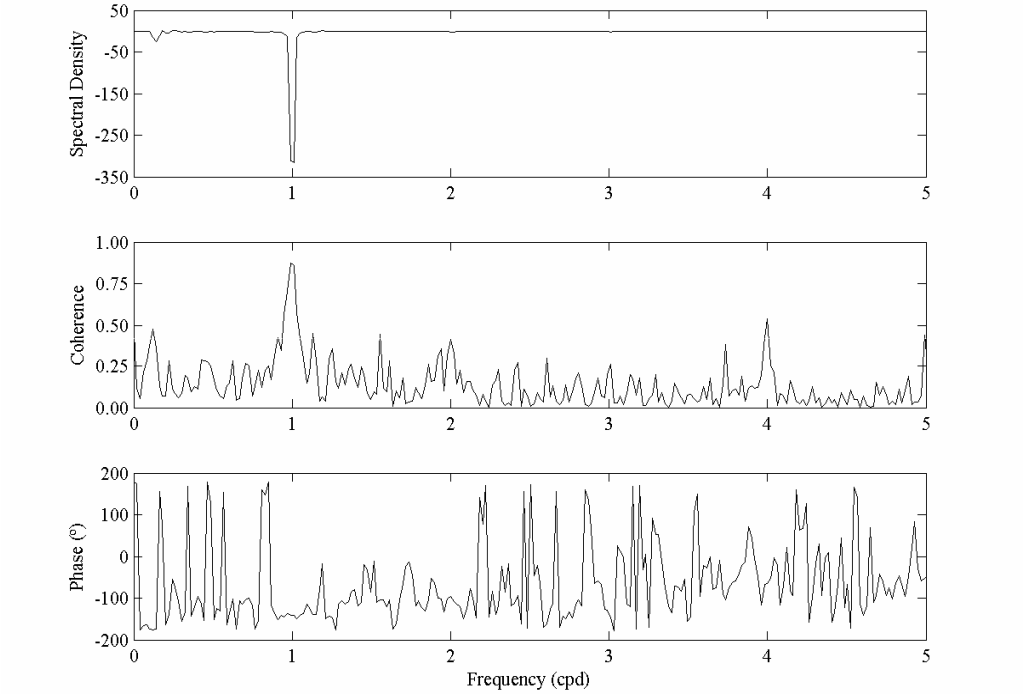

Figure 5.18: Cross spectrum, coherence and phase between the air temperature and the water temperature measured in the sensor 6.

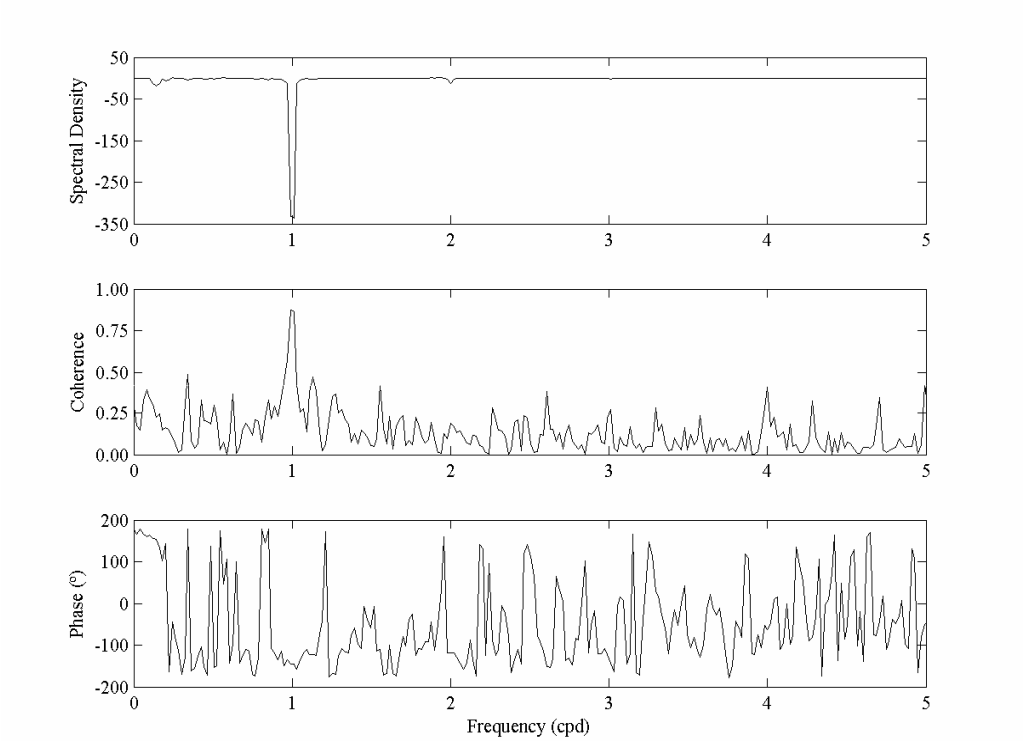

Figure 5.19: Cross spectrum, coherence and phase between the air temperature and the water temperature measured in the sensor 10.

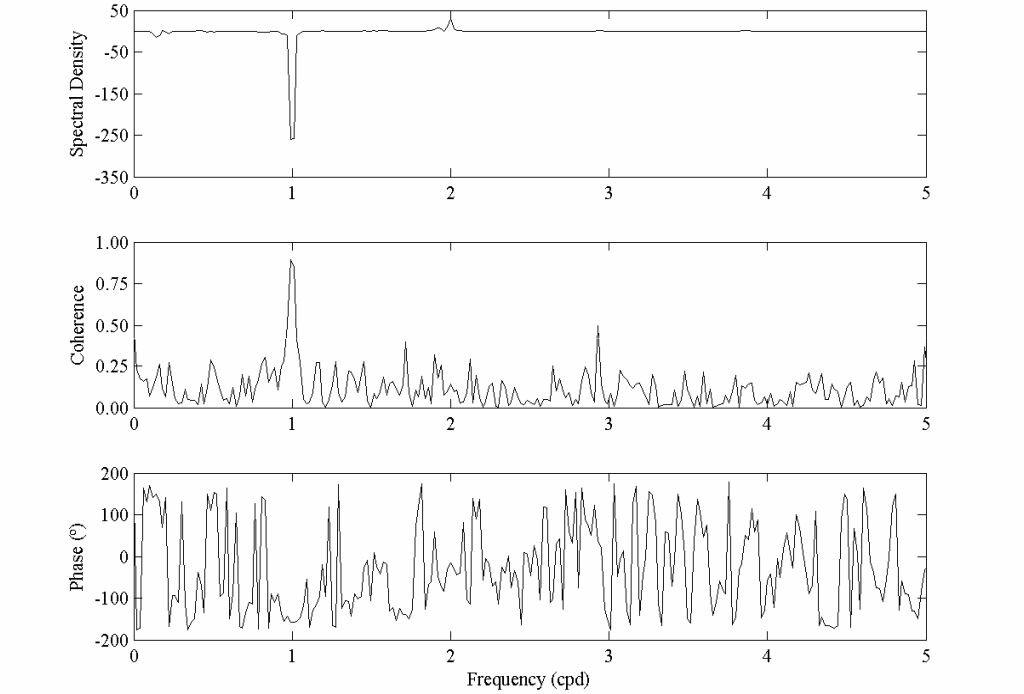

Figure 5.20: Cross spectrum, coherence and phase between the air temperature and the water temperature measured in the sensor 13.

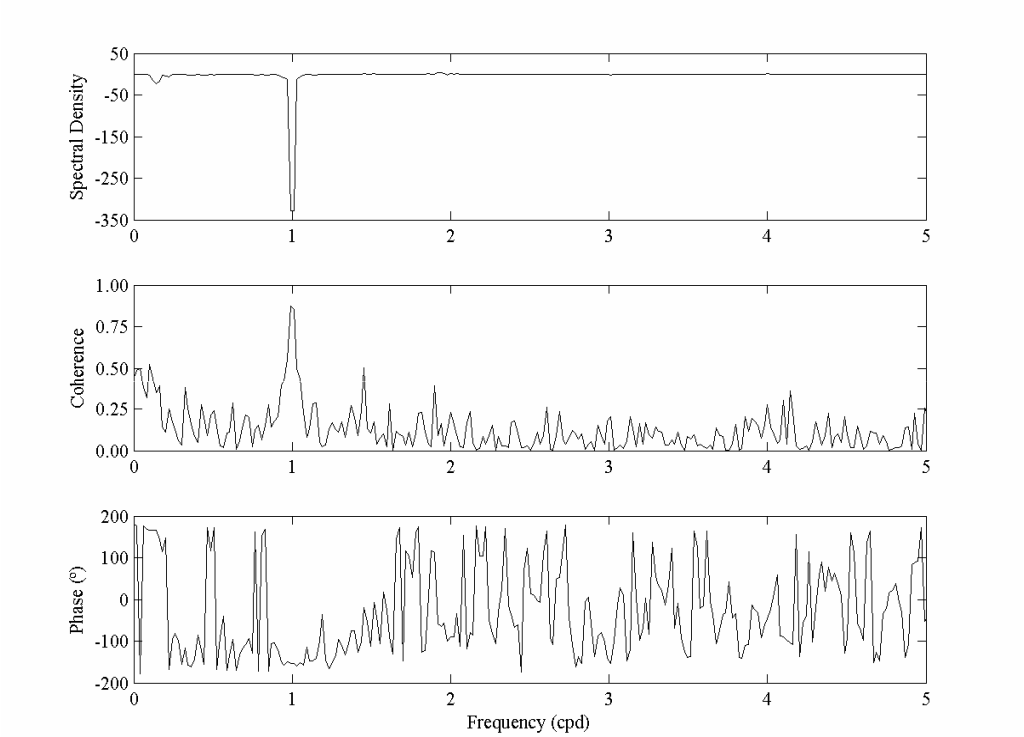

Figure 5.21: Cross spectrum, coherence and phase between the air temperature and the water temperature measured in the sensor 19.

5.3 Spatial- temporal variability

5.3.1 Seasonal variability

Figure 5.22 shows the spatial-temporal pattern of water temperature in the Espinheiro channel. Through the analysis of this figure, it can be observed that in Winter the channel's mouth presents higher water temperature values than the channel's head. In the Summer months the channel's head presents smaller water temperature than the mouth, as revealing a tendency opposed to what would be expectable. This may be explained by the fact the river flow was very low during the period under analysis. Then, the colder waters of the ocean mixed with the estuarine water in the channel's head, causing a decrease of the water temperature in that area.

It may be observed that the oceanic water temperature has a larger annual variability when compared to the seasonal fluvial water temperature variability, which presents a smaller range.

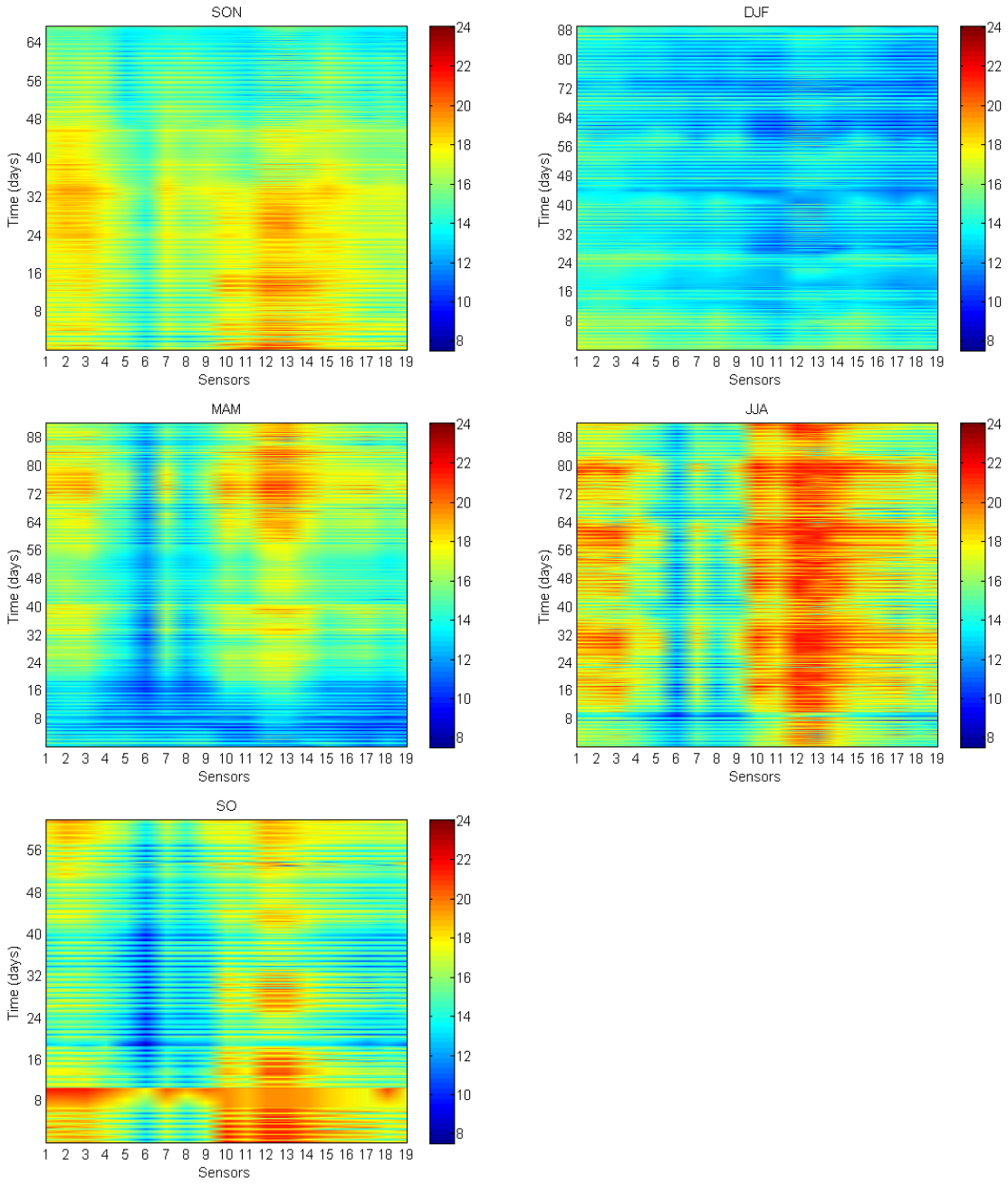

Figure 5.22: Seasonal representation of the water temperature variability. Color bar shows temperature in (ºC).

From Autumn to Winter, the water temperature in the inner part of the channel decreases almost 5 ºC, from values between 16 and 18 ºC to values between 11 and 13 ºC. This effect can be due, not only to the temperature of the ocean and river waters but also, to the decrease of the air temperature (Figure 4.1) and the shallowness of these areas. A similar result was found by Uncles and Stephens (2001) in the Tamar estuary.

In Winter, the water temperature is nearly constant along the channel. The observations show higher temperatures near the mouth (sensor 1) and lower temperatures in the upstream zone of the channel.

From Winter to Spring the water in the inner part of the channel becomes warmer increasing from about 11 ºC to 17 ºC at the end of the Spring. At this time of the year, the air temperature starts to increase (see Figure 4.1). This may be due to an increase in the air temperature and solar radiation.

In fact, starting from the middle of Spring to the middle of Autumn, warmer fluvial waters (sensor 19) enter the channel. The opposite occurs during colder seasons when warmer waters come into the channel from the sea. Near the fluvial region of the channel, the water temperature values are always 2 ºC warmer or cooler, depending on the year season, than in the rest of the channel.

The water temperature recorded by sensors 6 and 8 is low independently of the month (around 12 ºC).

In Summer, the water temperature within the channel increases to values higher than 24 ºC in sensor 13, which can be due to the fact that it is located in a shallow area (Figure 3.2), reflecting the influence of the solar radiation daily variability. The oceanic and fluvial boundaries of the channel have similar water temperature variations. This result is in agreement with Vaz and Dias (2008) for Autumn and Winter seasons.

Through the analysis of Figure 5.22, it may be verified that, for all seasons, the warm or cold waters reach up to sensor 3.

In order to verify the influence of the tide in transporting the ocean water into the estuary during the spring and neap tide in Winter and Summer, the water level and the water temperature recorded in sensors 1, 3 and 7 are plotted in Figure 5.23 and Figure 5.24 for a 21 days-period in December 2004 and July 2005, respectively.

Observing these figures, the water temperature recorded in sensor 1 and 3 presents similar patterns and values, varying with the tide (due to the proximity of the mouth), both in Winter and Summer. The daily variation in water temperature is also related to the tidal amplitude (the low tide produces an increase in water temperature) (Newton and Mudge, 2003). The water temperature increases at ebb tide and decreases at flood tide. However, in sensor 7 the tidal effect begins to attenuate, as it is already located 3 km from the mouth. This attenuation increases along the channel.

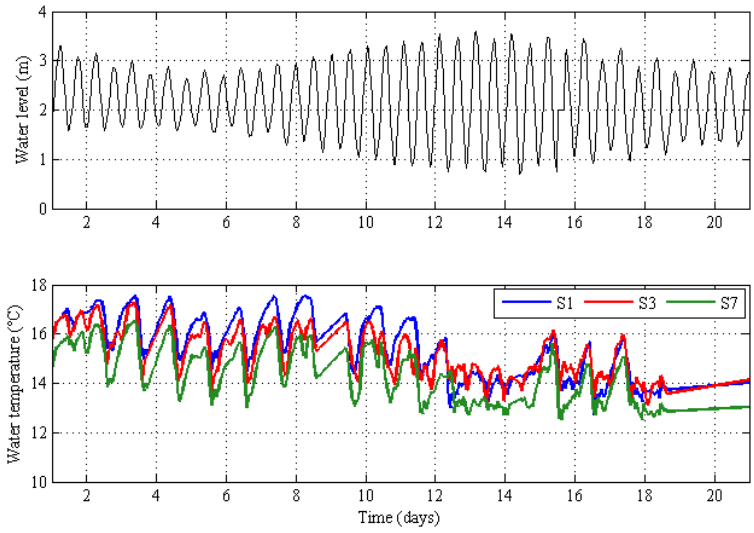

Figure 5.23: Water level (panel 1) and water temperature (panel 2) at sensors 1, 2 and 7 for December 2004.

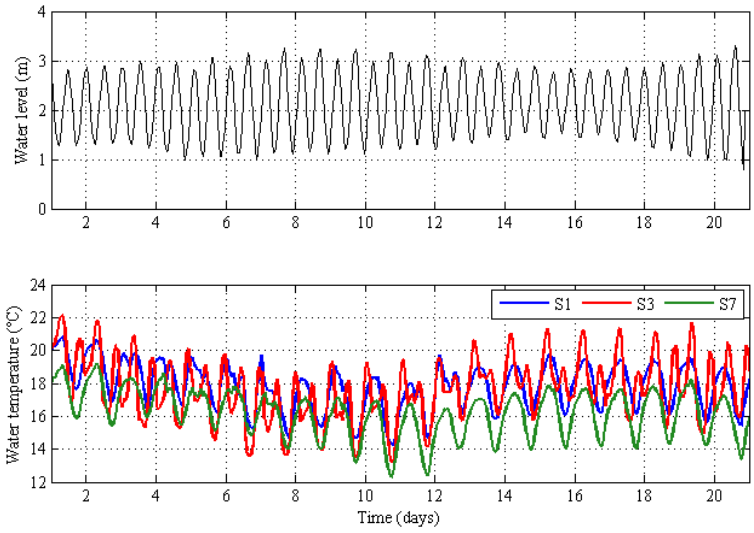

Figure 5.24: Water level (panel 1) and water temperature (panel 2) at sensors 1, 2 and 7 for July 2005.

From Figure 5.23 and Figure 5.24 it can be observed that the maximum tidal range of 3 m, which represents spring tide conditions, causes a small decrease, approximately 1.5 and 2.5 ºC in water temperature at sensors 1 and 3, respectively. A decrease in the tidal range, representing neap tide conditions, causes an increase about 3 ºC in water temperature data. This fact may be explained by the smaller velocities in neap tide, which causes a minor water renovation along the channel. But, the decrease in tidal range during neap tides results in a shorter tidal excursion within the channel.

In spring tide conditions, the tidal excursion extends along the entire channel on the flood tide. However, at 3 km into the channel, the tide begins to attenuate and it continues to decrease towards the channel's head.

The tidal range is considered an important factor for the differences in the water temperature along the channel. These results confirm the ones obtained in Tomales Bay (Harcourt-Baldwin and Diedericks, 2006) where the tidal range influenced the development of a density intrusion, where the tidal range controls whether the cold, dense water reaches the plunging area and in so doing, influences whether a density current does or does not develop.

As previously observed, the tidal range has an important role in the water temperature variation along the channel, mainly in areas near the mouth. Therefore it is thus appropriate to look to the sea surface temperature values, as they are also likely to have a signature in the temperature inside the channel. With the purpose of verifying the influence of the sea surface temperature in the values recorded by the sensors near the mouth of the lagoon, Figure 5.25 shows the satellite images corresponding to the study period presented in this section.

According to Figure 5.25 there is warm seawater (around 18 ºC) propagating upstream on 15 June 2005 as confirmed by Figure 5.22, where the influence of this high temperature is observed up to sensor 3. The opposite is observed on 6 July 2005, when colder water (around 14 ºC) enters in the lagoon, being visible in all sensors data.

In Figure 5.25 (6 July 2005) a band of cold water (15-17 ºC) can be observed near the coast with a length and width of approximately 150 and 50 km, respectively. This may be due to upwelling events, which are related to northern winds (Figure 4.1). Probably, the cold, upwelled water intrudes on the channel with the flood tide (Figure 5.24), because during the flood a greater entrance of water flow occurs (Figure 4.3). The ocean water can be one of the driving factor that causes water temperature variability in the Espinheiro channel. This was also the case within the Tamar estuary (Uncles and Stephens, 2001).

In this way and to evaluate the influence of the sea surface temperature in the water temperature recorded by the sensor near the mouth, correlations were calculated based on time series data represented in Figure 5.26.

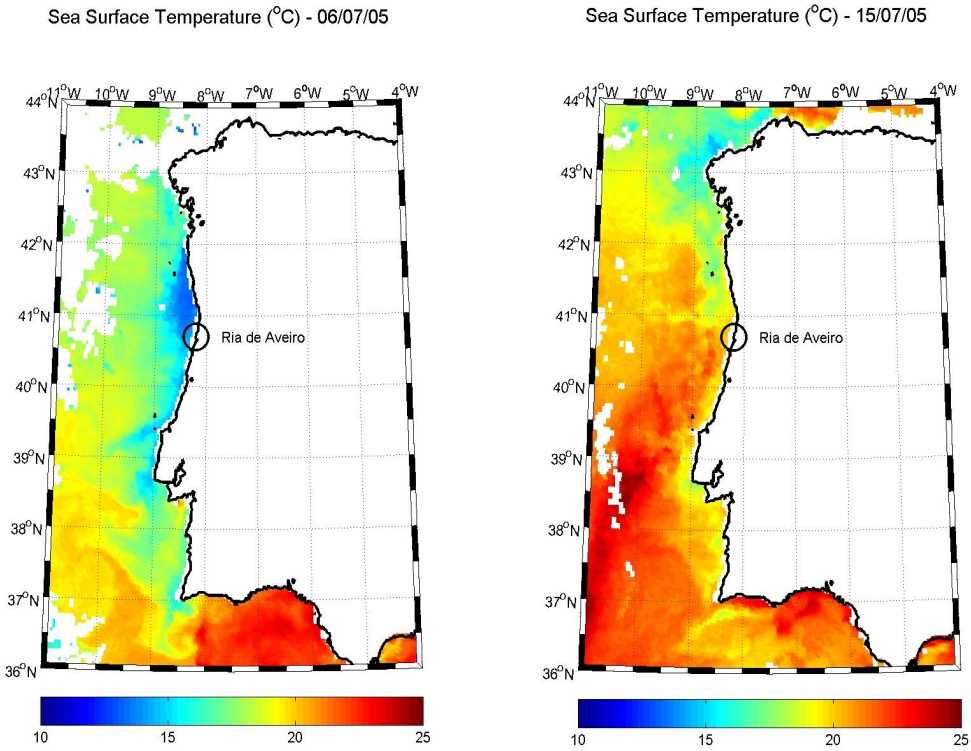

Figure 5.25: MODIS images of sea surface temperature.

The Figure 5.26 presents the similar behavior of the variables. The water temperature measured in sensor 1 between Julian days 152 and 188 is higher (about 0.5 ºC) than sea surface temperature. This difference can be due to the fact that a comparison between water temperature measured at a depth ~20 m and water temperature measured at the surface (satellite). This may also be a consequence of the weakness of the river flow, since the water column is completely filled with oceanic water (homogeneous water column) (Vaz and Dias, 2008).

In fact, the sea surface temperature is moderately correlated to the air temperature (0.6569) (as expected), because the solar radiation has a direct influence in the heating of the water. The sea surface temperature is strongly correlated to the water temperature measured in sensor 1 (0.9498) and sensor 2 (0.8878), showing a diminishing of the correlation towards the channel's head, which indicates that, due to the shallowness of the upper regions of the channel, the water temperature dynamics is also driven by the air temperature variation.

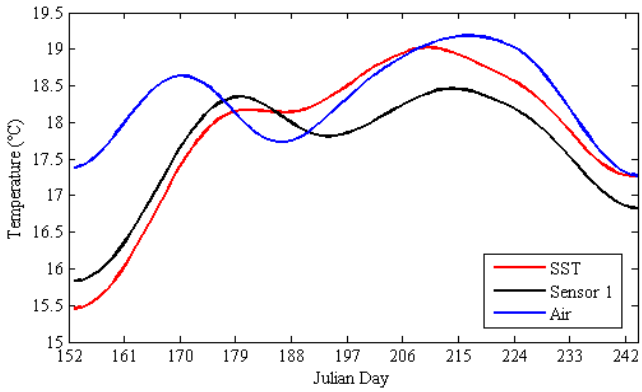

Figure 5.26: Time series of the sea surface temperature, water temperature measured in sensor 1 and air temperature.

5.3.2 Empirical Orthogonal Functions analysis

The decomposition of water temperature using empirical orthogonal functions (EOF) provides another method of analyzing the spatial and temporal components of water temperature variability. EOFs analysis is used to ascertain the most significant coherent mode of variation in the channel.

The highest coherent component (the first EOF) (Figure 5.27) explains 85% of the total variance of the water temperature inside the channel.

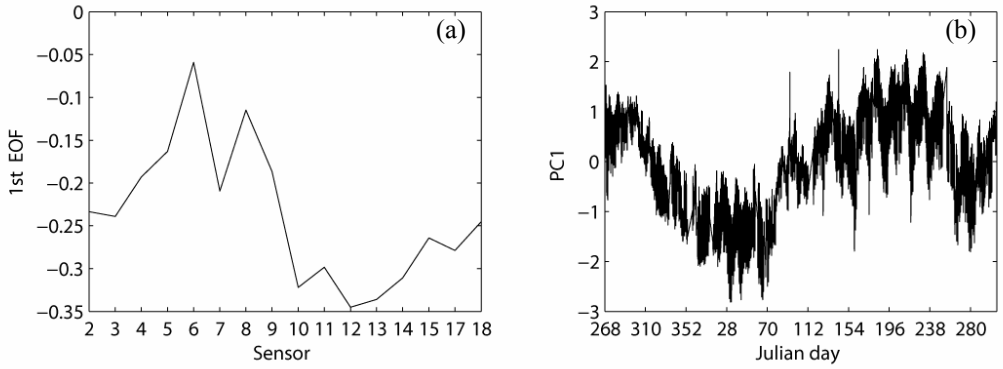

Figure 5.27: Spatial (a) and temporal (b) distribution of the water temperature first EOF.

The first Principal Component (PC1) (Figure 5.27b) is closely related to the inter-annual variation of the air temperature. The first EOF (Figure 5.27a) presents a non-homogeneous behavior along the channel. In sensors 6 and 8 are shown the smallest variation (the water temperature is low independently of the month) and sensors 12 and 13 show the highest variation (Figure 5.22). This may be a consequence of the air temperature

variation throughout the year. The correlations between the water temperature measured in the sensors and the PC1, and the correlations between the water and air temperature data are summarized in Table 5.1.

In fact, strong correlations were found between the temporal variation of the first EOF (PC1) and all water temperature data. Moreover, strong correlations were also found between water and air temperature. The exception is the correlations found at sensors 6 and 8. The PC1 is strongly correlated to the seawater temperature (0.9498) (sensor 1) and to the freshwater temperature (0.9560) (sensor 19), and is moderately correlated to the air temperature (0.6790).

Table 5.1: Correlations between the water temperature measured in the sensors and the PC1, and the correlations between the water and air temperature. Strength of correlation is defined as **Strong. |r|≥0.8; *Moderate. 0.5≤|r|≤0.8; Weak. r|≤0.5 (Reed *et al*., 2008).

Sensor	PC1	Air temperature
1	0.9498**	0.5338*
2	0.9579**	0.6285*
3	0.9342**	0.6136*
4	0.9231**	0.5386*
5	0.8289**	0.3510
6	0.3230	-0.3056
7	0.9118**	0.4848
8	0.5987*	0.0575
9	0.8842**	0.4267
10	0.9593**	0.7898*
11	0.9600**	0.8072**
12	0.9356**	0.8278**
13	0.9157**	0.8240**
14	0.9716**	0.7800*
15	0.9649**	0.6632*
17	0.9505**	0.6824*
18	0.9702**	0.6507*
19	0.9560**	0.6790*

The calculated correlations between air temperature and the water temperature time series are strong in sensors 11, 12 and 13; this may be a consequence of the shallowness of the region were sensors are located, in the way that higher influence from solar radiation can be found.

The water temperature distribution does not depend greatly on the river discharge, which presents lower values when compared to the typical values (Newton and Mudge, 2003) and it is closely related to the seawater temperature, tide and air temperature pattern.

6 Conclusions

The general purpose of this work was to analyze the water temperature variability in the Espinheiro channel and its relation to the main forcing mechanisms.

The results showed the importance of the major forcing factors (tide and meteorological conditions) that influence the water temperature behavior within the Espinheiro channel.

During the survey period, the water temperature variability presents maximum (minimum) values in sensor 13 (6 and 8). These peaks values may be related to the influence of the solar heating and also due to the fact that the water that leaves the São Jacinto channel could be colder than the water that comes from the upstream area of the Espinheiro channel.

The results for the Espinheiro channel clearly indicate that the oscillations of the water temperature are strongly related to the solar heating daily variation and the semidiurnal and diurnal tidal effect. On the other hand, the subtidal oscillations are dictated by the weather and/or meteorological long term events.

The spectral analysis (for the water temperature data) reveals high energy peaks in both semidiurnal and diurnal frequencies. These frequencies may be related to the daily variation of the air temperature and tidal forcing, demonstrating the importance of the meteorological variables in the modulation of the water temperature in shallow areas like the Espinheiro channel.

This study indicates that the harmonic analysis of the water temperature is an alternative way of estimating the importance of the tidal constituents along the channel.

The water temperature measured in sensor 2 (close to the lagoon mouth) showed the highest coherence (0.75) with the tide. This highest coherence revealed that heat is transported significantly from the nearly ocean. In spring tide conditions, the tidal excursion extends along the entire channel during the flood tide, causing the water temperature to decrease. However, at 3 km into the channel, the tide effect begins to attenuate and it continues to decrease towards the channel's head. In neap tide conditions, the water temperature increases about 3 ºC, but results in a shorter tidal excursion within the channel.

Results for the cross-spectral analysis obtained between the air temperature and water temperature showed that the solar radiation heating effect is important for the establishment of temperature patterns, especially in the shallow areas at the far end of the channel.

EOF analysis indicates that the variability in the water temperature time series can be accounted for by the first component, which is closely related to the annual variation of the air temperature.

The decrease in the correlation between the water temperature and sea surface temperature towards the channel's head indicates that, due to the shallowness of the upper regions of the channel, the water temperature dynamics is mainly driven by the air temperature variation in this zone. The depth of the channel is another important factor, where a decrease in the depth could result in an increase of the water temperature.

In conclusion, besides the dependence on the water temperature variation at the channel's boundaries (ocean and river), when the incoming freshwater is low (severe drought), the water temperature distribution is closely related to the meteorological conditions, like air temperature and incoming solar radiation, especially because of the shallowness of the Espinheiro channel. Specifically, near the mouth of the lagoon the water temperature is closely related to the tide and to the air temperature.

The results revealed that the fibre Bragg technology produces reliable results and therefore it can be used as a pre-operational system to monitor water properties like temperature in estuarine systems.

There are goals that remain for the future. Future work should be conducted to address the freshwater inflow data, in order to characterize the influence of the Vouga River freshwater inflow within the channel and evaluate the influence of the seasonal variation of freshwater inflow in the water temperature pattern inside the channel. Also, it should be interesting to carry out work in modeling in order to compensate the observations and in conjunction with data acquired in a continuous real time regime, it will allow the forecast of the lagoon evolution under critical conditions.

References

Abrantes, I., Dias, J. M., Rocha, F., 2006. Spatial and temporal variability of suspended sediments concentration in Ria de Aveiro lagoon and fluxes between the lagoon and the ocean. Journal of Coastal Research SI39, 718-723.

Aliani, S., Meloni, R., Dando, P. R., 2004. Periodicities in sediment temperature time-series at a marine shallow water hydrothermal vent in Milos Island (Aegean Volcanic arc, Eastern Mediterranean). Journal of Marine Systems 46, 109-119.

Armstrong, E. M., 1995. An Empirical Orthogonal Function Analysis of Spring-Summer Sea Surface Temperature Variability off Northern and Central California from AVHRR Satellite Imagery. Challenges of Our Changing Global Environment, Conference Proceedings 3, 2038-2045.

Atkinson, M. J., Allanson, B.R., Imberger, J., 1987. Fine-scale oxygen variability in a stratified estuary: patchiness in aquatic environments. Marine Ecology 36, 1-10.

Bjornsson, M., Venegas, S. A., 1997. A Manual for EOF and SVD Analyses of Climatic Data. Department of Atmospheric and Oceanic Sciences and Centre for Climate and Global Change Research, McGill University, CCGCR Report Nº 97-1, Montréal, Québec, 52 pp.

Cameron, W. M., Pritchard, D. W., 1963. Estuaries, in: The Sea. Hill, M. N. (Ed), John Wiley & Sons, New York, pp 306-324.

Dias, J. M., 2001. Contribution to the study of the Ria de Aveiro hydrodynamics. Ph.D. thesis, University of Aveiro, Portugal, University of Aveiro, 288 pp.

Dias, J. M., Lopes, J. F., Dekeyser, I., 1999. Hydrological characterization of Ria de Aveiro, Portugal, in early summer. Oceanologica Acta 22 (5), 473–485.

Dias, J. M., Lopes, J. F., Dekeyser, I., 2000. Tidal propagation in Ria de Aveiro Lagoon, Portugal. Phys Chem Earth (B) 25, 369–374.

Dias, J. M., Lopes, J. F., Dekeyser, I., 2001. Lagrangian transport of particles in Ria de Aveiro lagoon, Portugal. Phys Chem Earth (B) 26 (9), 721–727.

Dias, J. M., Vaz, N., Nolasco, R., Santos, J. L., Teixeira, M., Frazão, O., Soares, A., Monteiro Santos, F. A., Lopes, J. F., 2003. Tecnologias de Monitorização de Sistemas Marinhos: Aplicação à Ria de Aveiro (Portugal). II Congresso sobre Planejamento e Gestão das Zonas Costeiras dos Países de Expressão Portuguesa, CD-ROM, 5 pp.

Emery, W. J., Thompson, R. E., 1997. Data Analysis Methods in Physical Oceanography, Pergamon Press, 634 pp.

Fonseca, J. C., Janicas, M. G. R., Proença, M. C. G. F., 1988. Panaroma no Distrito, VII Jornadas de Saúde de Aveiro, Administração Regional de Saúde. Gráfestal, 222 pp.

Goto, S., Kinoshita, M., Mitsuzawa, K., 2003. Heat flux estimate of warm water flow in a low-temperature diffuse flow site, southern East Pacific Rise 17º25'S. Marine Geophysical Researches 24, 345-357.

Harcourt-Baldwin, J.-L., Diedericks, G. P. J., 2006. Numerical modeling and analysis of temperature controlled density currents in Tomales Bay, California. Estuarine, Coastal and Shelf Science 66, 417-428.

Hsu, M. H., Kuo, A. Y., Kuo, J. T., Liu, W. C., 1999. Procedure to calibrate and verify numerical models of estuarine hydrodynamics. Journal of Hydraulic Engineering, pp 166-182.

Kaplan, D. M., Largier, J. L., Navarrete, S., Guiñez, R., Castilla, J. C., 2003. Large diurnal temperature fluctuations in the nearshore water column. Estuarine, Coastal and Shelf Science 57, 385–398.

Keiner, L. E., Yan, X. H., 1997. Empirical Orthogonal Function Analysis of Sea Surface Temperature Patterns in Delaware Bay. IEEE Transactions on Geoscience and Remote Sensing 35 (5), 1299-1306.

Lopes, J. F., Dias, J. M., Dekeyser, I., 2001. Influence of tides and river inputs on suspended sediment transport in the Ria de Aveiro lagoon, Portugal. Phys. Chem. Earth (B) 26 (9), 729–734.

Moreira, M. H., Queiroga, H., Machado, M. M., Cunha, M. R., 1993. Environmental gradients in a southern estuarine system: Ria de Aveiro, Portugal, implication for soft bottom macrofauna colonization. Neth. J. Aquat. Ecol. 27 (2-4), 465–482.

Newton, A., Mudge, S. M., 2003. Temperature and salinity regimes in a shallow, mesotidal lagoon, the Ria Formosa, Portugal. Estuarine, Coastal and Shelf Science 57, 73–85.

Nolasco, R., Soares, A., Dias, J. M., Monteiro Santos, F. A., Palshin, N. A., Represas, P., Vaz, N., 2006. Motionally induction voltage measurements at estuarine environments: the Ria de Aveiro Lagoon (Portugal). Geophysical Journal International. doi: 10.1111/j.1365-246x.2006.02936.x.

Paraso, M. C., Valle-Levinson, A., 1996. Meteorological Influences on Sea Level and Water Temperature in the Lower Chesapeake Bay: 1992. Estuaries 19 (3), 548-561.

Pawlowicz, R., Beardsley, B., Lentz, S., 2002. Classical tidal harmonic analysis including error estimates in MATLAB using T TIDE. Computers and Geosciences 28, 929–937.

Reed, R. E., Dickey, D. A., Burkholder, J. M., Kinder, C. A., Brownie, C., 2008. Water level variations in the Neuse and Palmico Estuaries, North Carolina due to local and remote forcing. Estuarine, Coastal and Shelf Science 76, 431–446.

Reid, G. K., Wood, R. D., 1976. Ecology of inland waters and estuaries: New York. D. Van Nostrand Company, 485 pp.

Sepúlveda, H. H., Valle-Levinson, A., Framiñan, M. B., 2004. Observations of subtidal and tidal flow in the Río de la Plata Estuary. Continental Shelf Research 24, 509-525.

Sousa, M. C., Dias, J. M., 2007. Hydrodyanmic Model Calibration for a Mesotidal Lagoon: the Case of Ria de Aveiro (Portugal). Journal of Coastal Research SI 50, 1075 – 1080.

Thomas, A., Byrne, D., Weatherbee, R., 2002. Coastal sea surface temperature variability from Landsat infrared data. Remote Sensing of Environment 81, 262– 272.

Uncles, R. J., Stephens, J. A., 2001. The annual cycle of temperature in a temperate estuary and associated heat fluxes to the coastal zone. Journal of Sea Research 46, 143-159.

U.S. Environmental Protection Agency (USEPA), 1997. Volunteer Stream Monitoring: A Methods Manual. EPA 841-B-97-003. November. Office of Water, Washington, DC. 211 pp.

Vaz, N., 2007. Study of heat and salt transport processes in the Espinheiro Channel (Ria de Aveiro). Ph.D. thesis, University of Aveiro, Portugal, University of Aveiro, 151 pp.

Vaz, N., Dias, J. M., 2008. Hydrographic characterization of an estuarine tidal channel. Journal of Marine Systems 70, 168-181.

Vaz, N., Dias, J. M., Leitão, P., Martins, I., 2005. Horizontal patterns of water temperature and salinity in an estuarine tidal channel: Ria de Aveiro. Ocean Dynamics 55, 416–429, doi:10.1007/s10236-005-0015-4.

Vaz, N., Dias, J. M., Leitão, P. C., Nolasco, R., 2007. Application of the Mohid-2D model to a mesotidal temperate coastal lagoon. Computers & Geosciences 33, 1204-1209.

Wang, D., Chen, Z., Wang, J., Xu, S., Yang, H., Chen, H., Yang, L., Hu, L., 2007. Summer-time denitrification and nitrous oxide exchange in the intertidal zone of the Yangtze Estuary. Estuarine, Coastal and Shelf Science 73, 43-53.